NIOSH SBIR Phase II Final Progress Report

Basic Programmatic Data:

Principal Investigator:	Dr. Girish Srinivas; 303-940-2321 gsrinivas@tda.com
Contractor:	TDA Research, Inc. 12345 W. 52nd Avenue Wheat Ridge, CO 80033 (303) 422-7819
Project Title:	End-of-Service Life Indicator (ESLI)
Additional Contributors:	Drew Galloway (TDA), Dr. Steve Gebhard, P.E. (TDA), Mr. Jeff Martin (TDA), Dr. David Eisenberg (TDA), James Wilcox (AVON), Pete Daveridge (AVON)
Grant Number:	2R44OH009341-02A1
Distribution:	U.S. Government only; contains proprietary information Steve Dearwent **sed7@cdc.gov** TDA Project R-6201-003 **reports@tda.com**
Project Start Date:	9/1/2014
Project End Date:	8/31/2017
Period of Performance (this report):	9/1/2014 to 8/31/2017
Date of Report:	11/29/2017

SBIR Rights Notice (DEC 2007)
These SBIR data are furnished with SBIR rights under Contract No. 2R44OH009341-02A1. For a period of 4 years, unless extended in accordance with FAR 27.409(h), after acceptance of all items to be delivered under this contract, the Government will use these data for Government purposes only, and they shall not be disclosed outside the Government (including disclosure for procurement purposes) during such period without permission of the Contractor, except that, subject to the foregoing use and disclosure prohibitions, these data may be disclosed for use by support Contractors. After the protection period, the Government has a paid-up license to use, and to authorize others to use on its behalf, these data for Government purposes, but is relieved of all disclosure prohibitions and assumes no liability for unauthorized use of these data by third parties. This notice shall be affixed to any reproductions of these data, in whole or in part.

Table of Contents

List of Figures

List of Tables

List of Terms and Abbreviations

Table 1. Definitions, acronyms and abbreviations used in this report.

AVON	Avon Protection Systems, a global respiratory protective equipment corporation	**OPTO 22**	Computer-controlled automation control system
AWTCV	Automated Wind Tunnel Cooling Vent	**OSHA**	Occupational Safety and Health Administration
CBRN	Chemical, Biological, Radiological and Nuclear, (a level of protective measures)	**OV**	Organic Vapor
CDC	Centers for Disease Control	**PAC**	Programmable automation controller
CIE	Commission Internationale d'Eclairage	**ppmv**	parts per million volume, measure of the concentration of TICs in breathing air
ΔE_{ab}	Color change defined by the CIE L a b Color Space (see Appendix I)	**PU**	Polyurethane
ESLI	End of Service Life Indicator	**RH**	Relative Humidity
HEPA	High efficiency particulate air, a grade particulate filter	**ROPFM**	Randomly Oriented Polypropylene Fiber Mat, a type of plastic felt
K2A	Knowledge to Action, route to translate knowledge into action	**slpm**	Standard Liters Per Minute, volumetric flow rate of a gas corrected to standardized conditions of temperature and pressure
MFC	Mass Flow Controller	**TDA**	TDA Research, Inc.
MSA	Mine Safety Appliances, a global respiratory protective equipment corporation	**TIC**	Toxic Industrial Chemical
m^2/g	Meters squared per gram, surface area per mass unit of measure	**UV**	Ultraviolet light
NCCDPHP	National Center for Chronic Disease Prevention and Health Promotion	**VOC**	Volatile Organic Compound
NIST	National Institute of Standards and Technology	**V**	Version iteration numbering system, used to denote various prototype versions of the same system

Abstract

Project Title: End-of-Service Life Indicator (ESLI)

Principal Investigator: Dr. Girish Srinivas; 303-940-2321; gsrinivas@tda.com

No simple technology is commercially available that allows the user of a respirator to determine if the chemical protection capability of a respirator filter cartridge has been reduced by exposure during storage, or by saturation with gases while it is in use. As a result, many workers who are required to use respirator protection are at risk for chemical exposure because the filter cartridge change-out schedules are not reliable; surveys show that up to 30% of the users simply change their cartridge when they smell a breakthrough.

The 1998 OSHA revision to the standards for respirator cartridge use required that employers provide either a rigorous change-out schedule or require the use of a National Institute of Occupational Safety and Health (NIOSH)-certified end-of-service-life indicator (ESLI) for determining when a respirator cartridge needs to be replaced. Because no reliable, certified commercially available ESLI system has been developed, employers rely on respirator change-out schedules. These change-out schedules, however, are often inaccurate and unreliable due to the highly variable inputs used to calculate the lifetime of the respirator cartridges. As a result, wearers of the masks often do not follow the change-out schedules and are often exposed to chemical vapors prior to changing respirator cartridges. The Bureau of Labor Statistics and NIOSH surveys show that some 20-30% of all the workers determine their own respirator change-out schedules, which is against OSHA regulations.

To address this issue, TDA has developed and demonstrated a colorimetric ESLI that changes color in response to organic vapors, acid gases and basic gases. TDA incorporated it into prototype respirator cartridges with the help of our collaborators. Should this technology be incorporated into commercially available respirator cartridges, not only would ESLIs prevent incidental overexposure to vapors, but they would eliminate costly added expenses incurred from unnecessary replacement of *partially* used cartridges resulting from conservative change-out schedules. An effective technology would improve the safety of workers who use more than 12 million respirator cartridges annually in the U.S.

1. Section One

1.1 Significant or Key Findings

The ultimate goal of the End-of-Service Life Indicator (ESLI) project was to develop a manufacturable colorimetric ESLI prototype for respirator cartridges that reliably indicated expiration of the respirator cartridges' carbon beds for a large number of acid, basic, and organic vapors.

Figure 1 shows TDA's, snap-in, ESLI module and the injection molded filter cartridge that was designed to accept it. The components of the filter were assembled by our commercial partner, AVON, using commercial carbon filter cartridge assembly procedures and equipment. The colorimetric ESLI modules were assembled by hand at TDA's Table Mountain facility, although their components are amenable to automated production methods that would be similar to pH strip production methods.

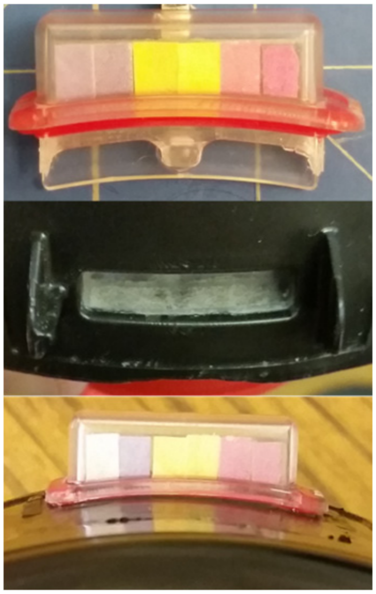

Figure 1. Top: ESLI module, Middle: ESLI port in filter cartridge, Bottom: ESLI module snapped into the filter cartridge port

TDA's multi-gas ESLI module consists of an array of three pairs of color-matched strips. The pairs of color-matched strips in Figure 1, from left to right, are: a bromocresol purple acid gas indicator and its purple reference strip, a brilliant yellow basic gas indicator and its yellow reference strip, and a sodium permanganate VOC gas indicator and its pink reference strip. In the lower panel of Figure 1, the ESLI module's bromocresol purple indicator has changed from purple to gray, indicating acidic vapor saturation of the first 70% of the filter cartridge's carbon bed.

The ESLI module works in conjunction with TDA's ESLI-enabled filter housing. The ESLI enabled filter housing has been designed to create a "slipstream" flow path through the ESLI module that ensures detection of contaminants when 70% of the carbon bed has become saturated. TDA's ESLI-enabled filter housings provide adequate time for color changes to be detected by signaling contaminant detection when 30% of the carbon bed remains in an unsaturated state. In most vapor contaminated environments, 30% of a filter's carbon bed equates to three hours of protection or more before contaminants pass through the bed to the user. Higher concentrations of contaminant gases cause more vibrant and rapid color changes in the ESLI module's colorimetric indicators, which would increase users' chances of detecting color changes.

1.2 Translation of Findings

TDA's ESLI technology was developed during a discovery study and would be categorized as being in the research phase of the CDC's NCCDPHP's K2A framework.

However, the materials, methods of construction, and the procedures for using TDA's ESLI-enabled filter cartridges are so inexpensive and self-explanatory that our commercial partner, AVON, could theoretically replace their commercial HEPA/carbon filter cartridge offerings with ESLI-enabled ones for, an estimated, $1 price increase per filter cartridge (retail pricing).

Purchase of ESLI-enabled filter cartridges sold by an AVON-TDA partnership would satisfy OSHA 1998's requirement that employers provide ESLI-enabled filter cartridges and supersede the requirement to provide change-out schedules and the oversight required to estimate and maintain those schedules. Decision-to-Adopt by employers would place TDA's ESLI technology in the translation phase of the K2A framework.

1.3 Research Outcomes/Impact

The findings of this study provide formulations for colorimetric indicators and a proven design for an indicating cartridge that could eliminate approximately 3.6 million exposures to contaminant vapors that occur each year when users of carbon-based filter cartridges delay cartridge replacement until they smell or taste contaminant vapors

2. Section Two

2.1 Scientific Report

2.1.1 Executive Summary


Figure 2. ESLI module and filter cartridge after acidic vapor testing

TDA Research, Inc. (TDA) and Avon Protection (AVON) have collaborated to develop and test a colorimetric End of Service Life Indicator (ESLI) for activated carbon cartridges used on personal respirators (Figure 2). The goal of the Phase II project was to develop and test a passive, colorimetric ESLI incorporated into a full-scale prototype activated carbon bed respirator filter cartridge. Activated carbon-filled respirator cartridges have been used as adsorptive filters in gas masks since the early 1900s (Mantell 1951), but a persistent drawback is that there is no simple way to know if the chemical protection capability of a respirator cartridge has been compromised (Favas 2005). The respiratory protection industry needs a simple device that indicates when a respirator cartridge is either used up or unsuitable for use. The ESLI will be built into the respirator cartridge as part of the original manufacturing process (it is not an add-on component), and in fact must be incorporated during manufacturing in order to obtain NIOSH certification.

Integrating a device into the activated carbon filter that changes color just prior to exhausting the capacity of the activated carbon is one way to indicate that no capacity remains for removing hazardous vapors from the atmosphere. Several non-hazardous, chemical colorimetric indicators currently exist that undergo a high-contrast color change when exposed to a large variety of toxic industrial chemical (TIC) vapors, including volatile organic chemicals (VOCs), acid gases, and basic gases. By integrating these indicator chemicals into an array, a visual ESLI can be constructed that allows the user of the gas mask to unambiguously determine if the capacity of an activated carbon respirator cartridge is approaching saturation. In TDA's design, the ESLI is a thin band of indicators that extends beyond the cylindrical boundary of the carbon-filled filter cartridge. A layer of activated carbon between the ESLI module's outlet and the filter cartridge's exit gives the user time to replace the cartridge with a new one when the ESLI indicates that the current cartridge's carbon bed is approaching saturation. The carbon filter's plastic housing has been designed to accept an ESLI indicator module that the mask user would insert into the filter housing's ESLI indicator port when the carbon filter is placed into service. In this configuration, as the carbon reaches its adsorptive capacity and vapors begin to break through (this is well before the bed is totally saturated) the vapors react with the indicators, producing color changes that indicate that the cartridge must be replaced.

2.1.2 Phase I results

In the Phase I project, with the help of our original commercial partner MSA, TDA successfully designed, fabricated, and demonstrated an ESLI prototype incorporated into an activated carbon-filled respirator cartridge. As part of the ESLI prototype's design and development, TDA selected appropriate colorimetric indicators for detection of the three major classes of TICs: VOCs, acid vapors, and basic vapors. Following the loading of these indicators onto compatible support (substrate) materials, the indicators' sensitivity and color change magnitudes were evaluated using the CIE Lab quantitative color system (CIE, 1986), described in section 2.1.6, using a range of contaminant gas concentrations under a variety of environmental conditions in which temperature and relative humidity were varied. Based on these results, TDA selected three colorimetric indicators for incorporation into its ESLI prototype – bromocresol purple (acid gas indicator), brilliant yellow (basic gas indicator), and sodium permanganate (VOC indicator). The choice of these three indicators in the prototype ESLI enables the ESLI to indicate that saturation of the gas mask's carbon bed has been reached for any of the three major classes of TIC vapors; for operation of this ESLI, if a color change of any of the three indicators is observed to change, the gas mask's activated carbon cartridge should be replaced. Following prototype fabrication, the prototype was demonstrated to respond to carbon bed saturation for all three vapor

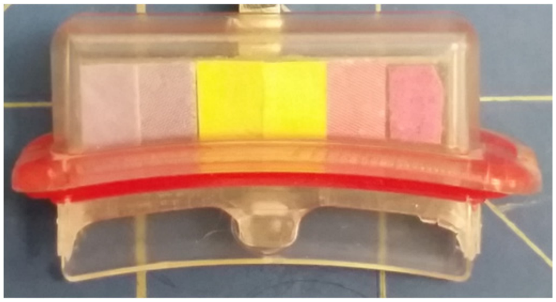
Figure 3. An injection-molded ESLI module

classes, as well as mixtures of vapor containing either VOC and acids, or VOCs and bases. During the testing and demonstration of the ESLI prototype, no mechanical failures of the device were observed and bed saturation was consistently indicated.

The successful fabrication and testing of TDA's ESLI prototype has demonstrated the effectiveness of an inexpensive, colorimetric ESLI for indicating the expiration of activated carbon respirator cartridges.

2.1.3 Purpose and Scope of the Phase II research effort

The standard for respirator cartridge use, OSHA 1998, required employers to provide either a change-out schedule or use a National Institute of Occupational Safety and Health (NIOSH)-certified end-of-service-life indicator (ESLI) for determining when a cartridge needs to be replaced (OSHA, 2011). Because no reliable, certified, commercially available ESLI system has been developed, employers have to rely on respirator change-out schedules. In a typical industrial environment where respirators are required, a production/safety manager is responsible for determining respirator cartridge change-out schedules using a "lifetime calculator," commonly found on a respirator manufacturer's website. These change-out schedules, however, are often inaccurate and unreliable because the manager must input highly subjective data (contaminant levels, breathing rates, etc.) (Rose-Pehrsson, 2005). Although the models are themselves accurate and tested, they rely entirely on subjective input from the safety manager because the model inputs are usually unmeasured estimates. Thus, it is very difficult to establish change-out schedules that fully protect respirator users from exposure to contaminants, and despite regulations, surveys show that ~30% of all workers determine their own change-out schedules (based on smelling the contaminants as they exit the respirator) (NIOSH/BLS, 2003).

In contrast, an effective, NIOSH-approved, ESLI technology that warns the user of impending contaminant breakthrough would provide an unambiguous means of safely determining when a respirator cartridge should be replaced; an ESLI would prevent incidental overexposure to vapors. Additionally, a reliable ESLI technology will eliminate costly added expenses incurred from unnecessary replacement of partially used cartridges resulting from early change-out schedules established from (rightfully) conservative lifetime estimates caused by mistrust of the lifetime calculator results. An effective ESLI technology would improve the respiratory safety of approximately 12 million respirator filter cartridge users in the U.S. annually.

2.1.4 Technical Progress

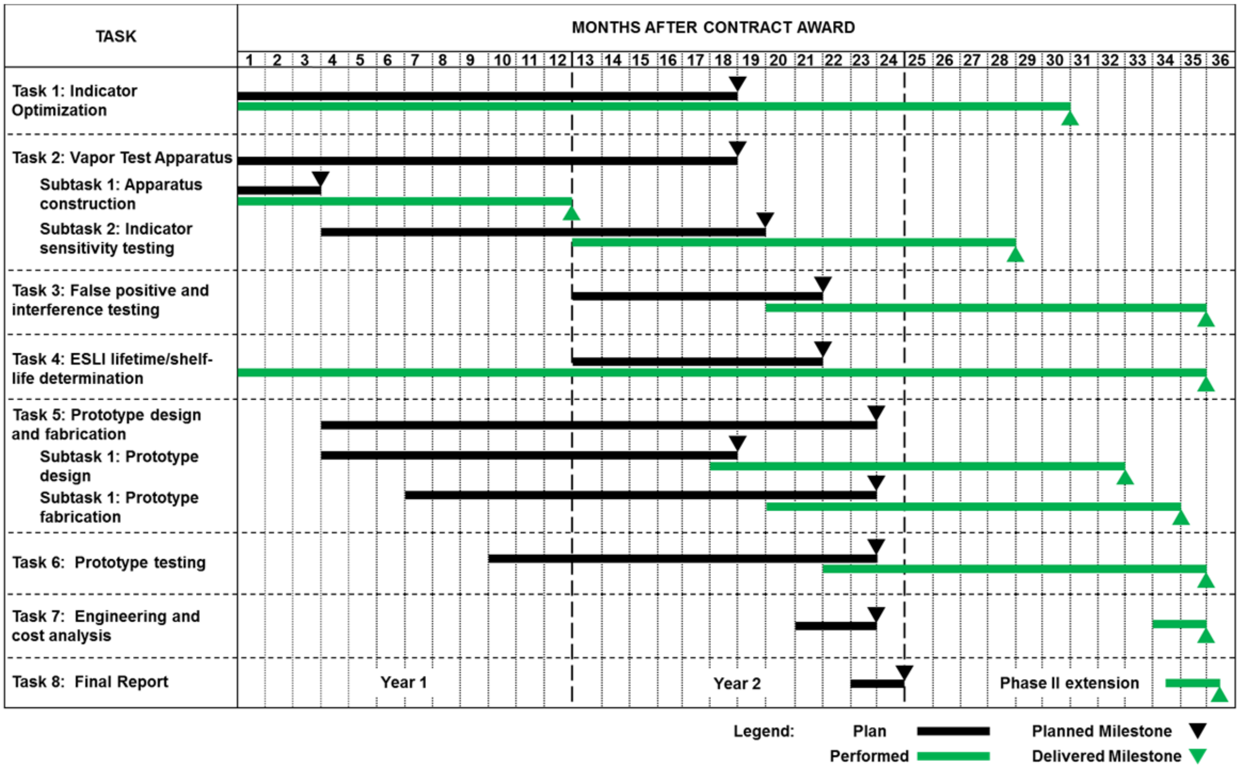

Figure 4. The Phase II ESLI project's schedule showing planned and actual efforts

Figure 4 shows the original Phase II project's schedule in black bars and milestone markers, while the actual project schedule over the extended period of performance is shown in green. The original, two-year, Phase II project schedule was extended by one year due to construction delays and technical issues. Construction of the vapor testing apparatus, Task 2 - Subtask 1, took longer than we had planned when we were forced to fabricate a new filter cartridge testing chamber, and an effort to solve the ESLI indicators' stability issues extended Task 1's duration by a year.

2.1.4.1 Task 1: ESLI indicator optimization

In this Task we optimized our indicator formulations for activity and stability, with a major focus on improving the indicators' shelf-lives. Striking the right balance between activity and stability will be crucial to the development of a commercial, passive, colorimetric ESLI. This task was performed before the other tasks so that indicators would be available for shelf-life testing, as well as prototype fabrication and vapor testing.

2.1.4.1.1 Background on the three ESLI indicator formulations

Goals of Task 1 were to optimize formulations for ESLIs (End of Service Life Indicators) for the detection of Volatile Organic Compounds (VOCs), acid gases, and basic gases.

Specific VOCs targeted in Phase II were: acetone, acetonitrile, benzene, cyclohexane, n-hexane, isopropyl alcohol (IPA), methanol, methyl isobutyl ketone (MIBK), trichloroethylene (TCE) and toluene. Targeted acid gases were HCl and SO_2, and the target basic gas was ammonia, NH_3.

2.1.4.1.1.1 Background on TDA's universal colorimetric VOC indicator

In order to be effective, the VOC indicators need to react and change color at concentrations of the toxic compounds near their Permitted Exposure Levels (PELs), which are typically in the ppmv range (for example, 400 ppmv for isopropyl alcohol). Color must change in time frames that allow the respirator to retain ~20% of its remaining lifetime. To be compatible with the respirator sorbent shelf life of >3 years, another goal is to optimize packaging and packaging conditions to allow long-term storage of the ESLI. The permanganate ion, MnO_4^-, was chosen as the universal color indicator for VOCs. It has a high oxidation/reduction potential of 1.679 eV when converted into MnO_2, allowing it to react with a very wide variety of oxidizable compounds, including SO_2, HCl and NH_3, according to the literature (see Purafil's web site). Color change of MnO_4^- is from purple/pink to the brown/beige of MnO_2.

To maximize the shelf life of colorimetric permanganate indicators they need to be protected from photochemical decomposition. The photochemical decomposition of the permanganate ion, MnO_4^-, is well understood (see Lee, et al., 1987; Nakai and Nakatsuji, 1994; Nakai, Ohmori and Nakatsuji, 1995). Photodecomposition proceeds with the evolution of molecular O_2 by the reaction: $MnO_4^- + h\nu \rightarrow MnO_2^- + O_2$. From the fundamental Grotthuss–Draper Law, only wavelengths of electromagnetic radiation that are absorbed by a system can bring about a photochemical change. From the literature, it is well documented that the photodecomposition of the permanganate ion is induced by absorption in wide bands centered in the UV at 311 nm (3.99 eV) and in the visible at 546 nm (2.27 eV). It is significant that the latter is near the maximum intensity of the solar radiation spectrum (Figure 5). Although the UV wavelengths might be filtered, absorption at 546 nm gives the permanganate its distinct purple/pink color, and it would not be straightforward to filter this wavelength without greatly altering the colored appearance of the indicator. Although the γ-alumina absorbs some of the wavelengths co-absorbed by permanganate in the UV, the substrate provides limited protection from photo-decomposition.

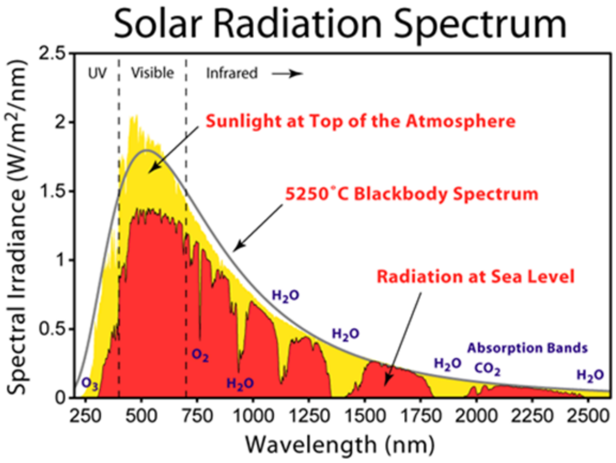

Figure 5. The solar spectrum at sea level relative to that at the top of the atmosphere, showing wavelengths and relative intensities of solar radiation to which ESLIs might be exposed. Note maximum near ~500 nm

According to Nakai and Nakatsuji (1994), the absorption at 546 nm produces a 1^1T_2 photoexcited state and absorption at 311 nm produces a 3^1T_2 excited state. Both of these initial photoexcited states are converted into the identical 1^1A_2 excited state, through which photodecomposition occurs (Nakai and Nakatsuji, 1994). According to Nakai, Ohmori and Nakatsuji (1995), the shorter, more energetic, wavelength at 311 nm (3.99 eV), in the ultraviolet, is much more photoactive relative to the shorter wavelength at 546 nm (2.27 eV), in the visible range.

Photodecomposition of permanganate has long been recognized. To increase shelf life, permanganate compounds are typically sold in dark-brown bottles, transmitting radiation only in the red, or in opaque barrels of thick polyethylene—the latter which is sufficiently inert to resist oxidation by permanganate. According to Cotton and Wilkinson, 1980, p. 747, (Wilkinson, Nobel Prize in Chemistry, 1973) the permanganate ion is stable in neutral or slightly alkaline media, and in the dark, decomposition is immeasurably slow. They state that permanganate solutions always should be stored in dark bottles.

In principle, the permanganate indicator should have indefinite shelf life provided that it is protected from light until actual use and if its substrate with condensed water is slightly alkaline. However, it will rapidly photo-decompose if exposed to the maximum of solar radiation at 546 nm and if a substrate with condensed water becomes acidic.

It should be noted that photodecomposition is of general concern for colorimetric indicators, not just the TDA materials. In colorimetric ESLIs sold by 3M Company, which employs, in part, nano-silver, photosensitivity is mitigated by using dark-black masking tape placed over the transparent polymeric window of the respirator (see Figure 6). The black tape is peeled back when the color indicator needs to be viewed (Figure 6). Likewise, for ESLI use, the permanganate indicators will best be stored in light-tight environments until use with similar dark tape on the respirator and are best shielded especially from radiation near 311 nm and 546 nm, which induce the photodecomposition.

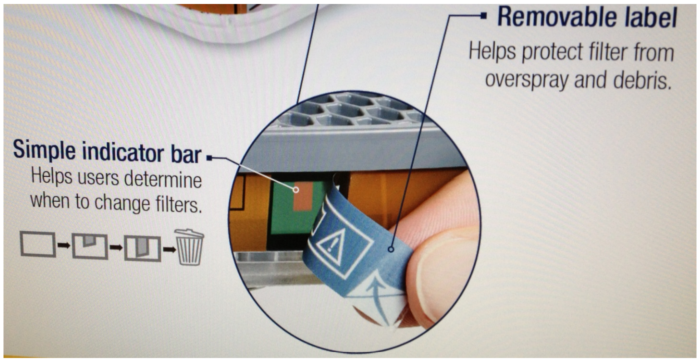

Figure 6. 3M's solution to photo-decomposition of their colormetric indicators is an opaque viewing port cover

For the universal, VOC (Volatile Organic Compound) colorimetric indicator, the permanganate ion, MnO_4^-, adsorbed onto activated, high-surface area γ-alumina was chosen as the support for permanganate. The γ-alumina material is a well-established support for permanganates used in the oxidation of organic materials and is used commercially in air purifiers (see Purafil's website). The γ-alumina is also a well-established desiccant and drying agent, readily chemisorbing water at Lewis acid sites and physisorbing water through hydrogen bonding at polar hydroxyl (--OH) surface sites. According to Lee, Chen and Wang, 1993, water is a critical component in the oxidation mechanism of permanganate and must be present to initiate steps in the conversion of MnO_4^- into MnO_2. According to Lee, Chen and Wang, 1993, the Lewis acidity of γ-alumina is critical for the adsorption and subsequent oxidation activity of the permanganate. Supports such as bentonite, with weaker Lewis-acid sites, do not function as well. The γ-alumina is also widely used in petroleum cracking catalysts and adsorbs a wide variety of organic substances. In addition, activated γ-alumina adsorbs almost all classes of organic compound to some degree except some saturated aliphatic hydrocarbons. However, the latter may react directly with adsorbed permanganate.

By far the best support for colorimetric permanganate indicators that we found is a γ-alumina (NorPro® SA-6176) produced by Saint-Gobain. This γ-alumina has a relatively high surface area of 250 m^2/g and an exceptionally high porosity and pore-size distribution in the 300-800 nm range. Upon activation at 400°C, it retains the γ-alumina crystal structure (verified by x-ray diffraction at TDA) and readily adsorbs 0.04 M aqueous MnO_4^-, with the MnO_4^- ions binding to the Lewis acid sites of Al, according to the literature. Sodium permanganate, $NaMnO_4$, rather than the more common $KMnO_4$ is preferred due to its much higher solubility in water ($9.0\ g{\cdot}L^{-1}$ vs. $0.64\ g{\cdot}L^{-1}$), lower probability of precipitating and closing pores of γ-alumina, and its deliquescent properties that attract the atmospheric water necessary for the permanganate oxidation reactions. When stored in the dark and *under neutral or slightly basic conditions,* decomposition of permanganate is reported to be immeasurably slow, whereas under acid conditions, decomposition is accelerated. The aqueous supernatant of γ-alumina + 0.04M $NaMnO_4$ is made slightly basic (pH = ~8.2) by adding 0.04 M $NaHCO_3$, which also acts as a buffer. From equilibrium considerations, the $NaHCO_3$ also limits uptake of atmospheric CO_2 that otherwise could dissolve in adsorbed water to form acidic H_2CO_3. Preparation temperatures are kept well below ~50°C to minimize decomposition of $NaHCO_3$ to the much more basic Na_2CO_3, which also can lead to decomposition of permanganate. As the permanganate indicator is designed to react with ppmv levels of organic compounds and is susceptible to photo-decomposition, the permanganate must be stored in highly vapor-impermeable, light-tight containers to minimize premature color change.

Permanganate does have limits to its oxidizing capabilities. Very stable organic molecules including acetonitrile, benzene and trichloroethylene (TCE) are simply too stable to react with permanganate under the conditions within respirators, and in fact are often used as refluxing solvents to dissolve permanganate when it is used to oxidize various organic molecules in organic synthesis reactions.

2.1.4.1.1.2 Background on TDA's acidic vapor indicator

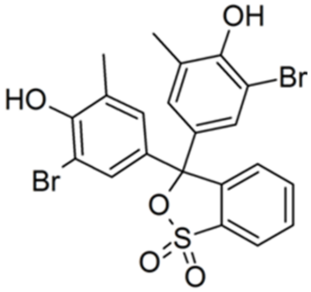

Figure 7. Bromocresol purple is purple above pH = 6.8 and yellow below pH = 5.2

Bromocresol purple was chosen as the acid indicator because it readily changes color from purple at pH >6.8 to yellow at pH <5.2—a range that is relatively unaffected when H_2CO_3 forms via dissolution of CO_2 into water. It is converted into its basic, purple form by adjusting pH to ~6.8 with NaOH. A basic solution is adsorbed onto Whatman #4 cellulosic filter paper along with hygroscopic LiCl, which attracts and retains the water necessary to allow ionization of the bromocresol purple as well as promote the transport of protons (H^+) produced by acid gases (HCl, SO_2) that react with water to release H^+. At pHs less than 5.2 bromocresol purple is converted into its yellow, acidic form by proton binding. The bromocresol purple indicator appears gray when mixtures of the purple and yellow forms co-exist in the pH range between 5.2 and 6.8. Bromocresol purple is photosensitive, and as with the permanganate indicator, is best stored in the dark.

The photo-induced decolorization of bromocresol purple is also well established. Photo-induced decolorization of this organic dye occurs by disruption of the conjugated system of double bonds that give rise to its intense color. This occurs not only by photo-cleavage of these and other bonds in the molecule, but can occur also by photoisomerization or by addition reactions across the system of double bonds. Bromocresol purple, in its basic form at pH >6.8, absorbs strongly in a wide band centered near 588 nm (Belattar, et al., 2014; El-Ashgar, et al., 2012), which, like permanganate, is also near the solar maximum. However, as in the case of the permanganate, this wavelength cannot be filtered to prevent photochemical reactions as it is responsible for the indicator's color. In the acid form at pH <5.2, absorption occurs in a band centered at 432 nm. The dye is easier to photodegrade in the acid form, which absorbs the more energetic photons at 432 nm (Akpan and Hameed, 2009). Both bands at 588 nm and 432 nm are present between pH = 5.2 to 6.8. However, in the TDA ESLI, this dye would be stored in the basic form at pH >6.8. Absorption at 432 nm and photochemical reactions induced at this wavelength are less of an issue.

Bromocresol purple also absorbs in the UV in a band centered near 276 nm and absorbs very strongly at wavelengths shorter than ~250 nm (Belatar, et al., 2014). These wavelengths will be of relatively low intensity in the solar spectrum (Figure 5). However, common fluorescent lamps employ Hg, which emits at 253.7 nm and could induce photochemical reactions in bromocresol purple. In addition, bromocresol purple is photo-degraded by highly reactive hydroxyl radicals, OH·, produced by photo-catalysts containing, for example, Fe, Cu and Ti (see, Belattar et al., 2014; Akpan and Hameed, 2009; Tavakkoli, et al., 2014). Photo-catalysts, and especially iron, can be present as impurities. The photo-catalysts absorb at various wavelengths in the visible and UV. As with permanganate, for long-term storage, bromocresol purple is sold in containers blocking radiation more energetic than about 650 nm or in completely light-tight, sealed packages. As with MnO_4^-, the bromocresol purple is best stored under light-tight conditions and shielded from all UV and visible radiation until the indicators are ready to be placed in-service on an ESLI-enabled filter cartridge.

2.1.4.1.1.3 Background on TDA's basic vapor indicator

The dye, brilliant yellow, resists photo-decolorization when adsorbed onto Whatman #4 cellulosic filter paper with hygroscopic LiCl. It reacts readily with ammonia. However, this reaction is reversible and the indicator reverts to its original color when ammonia is removed. This could be an issue during intermittent exposures to ammonia.

During solar radiation testing at TDA, brilliant yellow retained 87% of its color after 4 h exposure to 800W solar-simulated radiation. This dye has λ_{max} = 398 nm (according to the Sigma-Aldrich web site) but is less sensitive to photo-decolorization than the other indicators. Nevertheless, photodecomposition was observed, so shielding the basic vapor indicators from UV and visible light would be beneficial to their shelf lives.

2.1.4.1.1.4 Optimizing the universal VOC indicator

The permanganate ion, MnO_4^-, was chosen as the universal color indicator for VOCs. It has a high oxidation/reduction potential of 1.679 eV when converted into MnO_2, which allows it to react with a very wide variety of oxidizable compounds. The color change from MnO_4^-'s purple/pink to the brown/beige of MnO_2 can be highly visible when it is diluted. Many permanganate counter-ions (Li^+, Na^+, K^+, Mg^{2+}, Ca^{2+}, Sr^{2+}, Ba^{2+}, Zn^{2+}, etc.) could have been chosen for use in the VOC indicators. $NaMnO_4$ was selected over the more common $KMnO_4$ for use as the colorimetric VOC indicator due to its much higher aqueous solubility: 900 g $NaMnO_4$/L vs. 63.9 g $KMnO_4$/L (20°C). $NaMnO_4$'s very high solubility eases dissolution during solution preparation and minimizes premature precipitation during indicator deposition.

Figure 8. MnO_4^- diluted with white, γ-alumina appears pink

$NaMnO_4$ is deeply colored in its crystalline form. The color change due to the reduction of the permanganate ion can be difficult to see when that change is from dark purple to dark brown. The color change can be much more visible when the permanganate exists as a thin layer on a white background. Then the color change is from the pink color shown in Figure 8, to beige.

Initially, we were working with potassium permanganate. However, its solubility in water was less than 1/10th of sodium permanganate's and therefore it restricted the range of aqueous solutions that could be deposited on the prospective VOC indicator's support materials. Sodium permanganate allowed us to expose, through drying, some less hydrophilic surfaces on the VOC indicator's support material in an attempt to attract hydrophobic vapors and improve reaction rates for the hydrophobic species of organic contaminants.

Permanganate solutions were deposited onto randomly oriented polypropylene fiber mats. As we had observed in the basic and acidic cases, that led to low viewable colored surface area and, more importantly, very low substrate stability. We deposited permanganate solutions on a range of support materials that were commercially available and would lend themselves to automated indicator fabrication. The permanganate solutions were reduced on every substrate that we deposited them on except for one. After attempting depositions on paper, polypropylene, alpha alumina, and silica, we created stable VOC indicators using gamma alumina as the diluent/support material. The gamma alumina that we selected was a high surface area catalyst support supplied by Norton, named SA-6176. With 250 square meters per gram surface areas the gamma alumina provided enormous surface areas for the deposition of permanganate solutions.

Literature describing permanganates as oxidizers for organics (Kuehner, 1954) recommended the addition of sodium bicarbonate at the same concentration as the permanganate to create a slightly basic environment for the oxidation of the permanganate.

Sodium permanganate was deposited on gamma alumina in concentrations from 1M to 0.0001M. The optimal $NaMnO_4$ concentration based on the ΔE_{ab} , see Appendix I for an explanation of ΔE_{ab} , and the sensitivity to VOCs was 0.04M.

To deposit sodium permanganate on the high surface area alumina, an aqueous solution of sodium permanganate and sodium bicarbonate was created by adding the sodium bicarbonate to boiling water to enhance its solubility. Once the sodium bicarbonate was completely dissolved, the solution was cooled and the sodium permanganate was added and allowed to dissolve. Finally, pellets of the gamma alumina were added to the solution. The gamma alumina pellets were allowed to soak in the permanganate solution for 30 minutes and then the solution was decanted and discarded. The wet pellets were placed in a beaker, capped with aluminum foil to limit exposure to the surrounding environment, and placed in a 45 C oven for 48 hours. The water content of the indicator material after drying was between 13 and 20 weight%. The water content of the sodium permanganate powder usually did not drop below 20 weight%. Also, in both cases (K and Na), there was always 4 weight% strongly bound water on the gamma alumina powder after the permanganate treatment that should not, according to the literature, play a role in the oxidation chemistry. Based on calculations, 12.9 weight percent H_2O would be required to produce a monolayer of water that covered the $250m^2/g$ surface area of the $NaMnO_4/\gamma$-alumina powder. Subtracting 12.9 wt% from the 20 wt% H_2O that remained in the average batch of $NaMnO_4/\gamma$-alumina powder leaves 7.1 wt% extra H_2O that was free to aid in aqueous reactions.

To create a homogenous powder compacts with even color, the indicator pellets were ground and sieved to -120 mesh and pressed into 1 inch discs with 1.5 mm thicknesses. The VOC indicator discs were stored in glass jars wrapped in aluminum foil until they were needed for testing. The room temperature shelf life of the indicator discs in glass jars, exceeded 24 months when they were protected from photodecomposition.

Our final formulation: 0.04M Sodium Permanganate, 0.04M Sodium Bicarbonate, DI Water, deposited on gamma alumina SA6176. After immersion in the permanganate solution the pellets were dried at 45 C in air.

2.1.4.1.1.5 Optimizing the acidic vapor indicator

Initially we were working with bromocresol green that does not complete its color change until pH 3.8. To increase the indicators' sensitivity to acidic vapors we switched to bromocresol purple.

To use bromocresol purple as an indicator for acidic gases we created dilute solutions and deposited them onto porous supports.

Our initial deposition efforts focused on using randomly oriented polypropylene fiber mats (ROPFMs) as substrates for the acidic gas indicator solutions. We determined, after several weeks of trials using varied concentrations of bromocresol purple, that the ROPFMs were poor substrates for the visual detection of color change. The open, fibrous nature of the ROPFMs provided a low viewable area when compared to filter paper.

Whatman #4 filter paper turned out to be an excellent substrate for viewing bromocresol purple. Its high viewable area, absorbency, gas permeability, and its bright white color all contributed to its selection as the substrate for the bromocresol purple indicator.

The literature describing aqueous solutions of bromocresol purple for use as acid indicators recommended fairly high concentrations of NaOH to stabilize the solutions. Our desire for the acid indicator paper to display high sensitivity to acidic vapors precluded using NaOH to create highly stabilized solutions of bromocresol purple. This conflict led to a set of experiments that determined the minimum NaOH content necessary for indicator stability in the dry form. For a 100ml batch of bromocresol purple solution with a bromocresol purple concentration of 0.0002M, an NaOH concentration of 0.008M permitted the conversion of six, six-inch discs of Whatman #4 filter paper into acid indicator paper. The relative amounts of NaOH to filter paper were important because the filter paper is acidic in its as-produced form.

Figure 9 shows the range of colors that are normally displayed by TDA's, bromocresol purple, acidic vapor indicators. Testing with PEL concentrations of SO_2 and HCl produce the color change indicated by the lower arrow in Figure 9. The acidic vapor indicator's transition from purple to gray is caused by the inability of the relatively dilute acidic challenge gas concentrations to produce pHs below 6.3 on the bromocresol purple indicators below 6.3. The gray color is produced by a fine mixture of purple and yellow regions. Exposure to much higher acid vapor concentrations produced vibrant yellows.

Bromocresol purple was deposited on filter paper in concentrations from 0.1M to 0.0001M. The optimal concentration for viewable color change was 0.0002M. It is of interest that the bromocresol purple and the brilliant yellow concentrations turned out to be the same. Our conclusion is that the 0.0002M concentration on white filter paper allows even distributions without the possibility for large amounts of recrystallization.

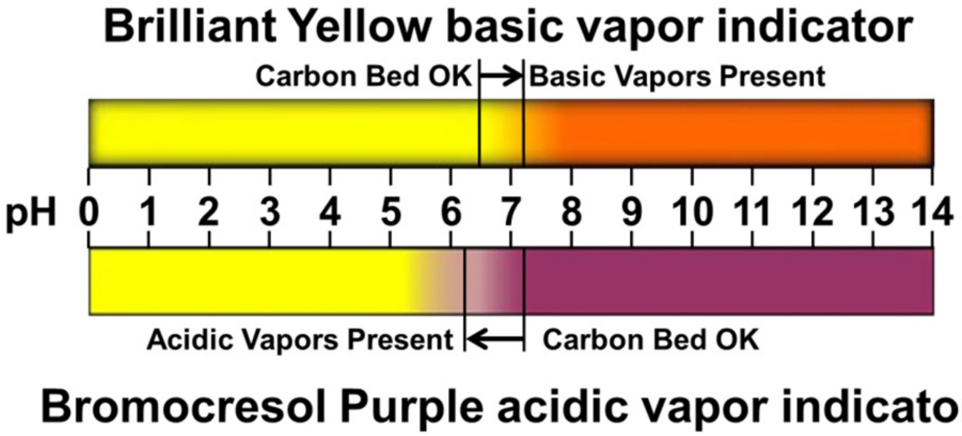

Figure 9. Color changes and pH ranges for TDA's, pH-based, colorimetric vapor indicators

To deposit bromocresol purple on filter paper an acetone/water solution was made and the filter paper was immersed in the solution for 20 seconds, the filter paper was removed from the solution and it was hung from a binder clip to promote drying in room temperature air.

During the early stages of the indicator preparation it was noted that the filter paper lost strength after exposure to the purely aqueous solutions. The mechanism for strength loss appeared to rely on the disentanglement of the filter paper's pressed fibers that commenced when the fibers became swollen with water and reached a terminal state when the paper had returned to pulp. To combat the loss of strength due to excessive water retention in the filter paper, 75% of the solution's water content was replaced with acetone. It was observed that acetone did not cause the filter paper to swell or disintegrate, that it was completely miscible with water and brilliant yellow, and had the added benefit of accelerating the filter paper's drying process after immersion in the dye solutions.

Very slow response was observed after the indicator papers were completely dry. We theorized that water was not present in enough abundance to allow the color change reaction to occur rapidly. To populate the indicator papers with non-fugitive water we added lithium chloride. The lithium chloride was added to the bromocresol purple solutions at concentrations from 10x to 1000x the bromocresol purple concentration of 0.0002M. Time-to-color-change experiments showed increased reaction rates upon addition of lithium chloride for levels up to 50x the brilliant bromocresol purple's concentration, followed by little increase in reaction rates at higher concentrations.

The acid indicator's final formulation was: 0.0002M Bromocresol Purple, 0.01M LiCl, 0.008M NaOH, 75% Acetone, 25% Water on Whatman #4 filter paper. After immersion in the bromocresol purple solution the filter papers were dried at room temperature in air.

2.1.4.1.1.6 Optimizing the basic vapor indicator

Brilliant Yellow, CAS# 3051-11-4, was chosen as the dye for the basic vapor indicators because its color change from yellow to red occured in the pH range from 6.5 to 8.

Solutions of Brilliant Yellow were initially deposited on ROPFMs. Unfortunately, the resulting basic vapor indicators were only faintly colored and made poor colorimetric indicators.

The brilliant yellow solutions were deposited on filter paper, making use of the same solution to the lack of color saturation that we discovered for the acidic vapor indicators. Without pH adjustment, the Whatman filter-paper-based, basic vapor indicators were stable in their yellow form. It can be difficult to measure the pH of solids, however, it appears that the basic vapor indicator sheets have a pH of 6.5, based solely on their sensitivity to ammonia vapors. The upper portion of Figure 9 provides a graphical representation of the basic vapor indicator sheet's working pH/color range during vapor testing.

LiCl was added to the basic vapor indicators' formulation when it was noted that the basic vapor indicators stopped working if they were allowed to dry completely. Tests identical to those performed with the acidic vapor indicators' formulation were carried out with the Brilliant Yellow basic vapor indicators' formulation and led to, interestingly, the same result. We concluded that properly loading the indicators with water had little to do with the dyes and was mainly a function of their substrate (the Whatman #4 filter paper).

The final basic vapor indicators' formulation was: 0.0002M Brilliant Yellow, 0.01M LiCl, 75% Acetone, 25% Water on Whatman #4 filter paper. (Dried in air at room temperature)

2.1.4.2 Vapor test apparatus

The purpose of this subtask was to create a carbon bed filter cartridge testing apparatus that would supply a stream of breathing air with tunable characteristics. The tunable characteristics of the breathing air stream were temperature, relative humidity, flow rate, and TIC concentration. The apparatus featured a filter testing chamber with a window that facilitated colorimetric indicator color change monitoring and recording.

2.1.4.2.1 Background: the Phase 1 ESLI testing apparatus

The Phase 1 apparatus that we built to test colorimetric indicator formulations was designed to expose colorimetric indicator coupons to precise concentrations of TIC vapors while controlling the challenge gas air stream's temperature, relative humidity and flow rate. We used rotameters to control the flow rates of the air stream's various constituents into mixing zones that preceded the sample chamber.

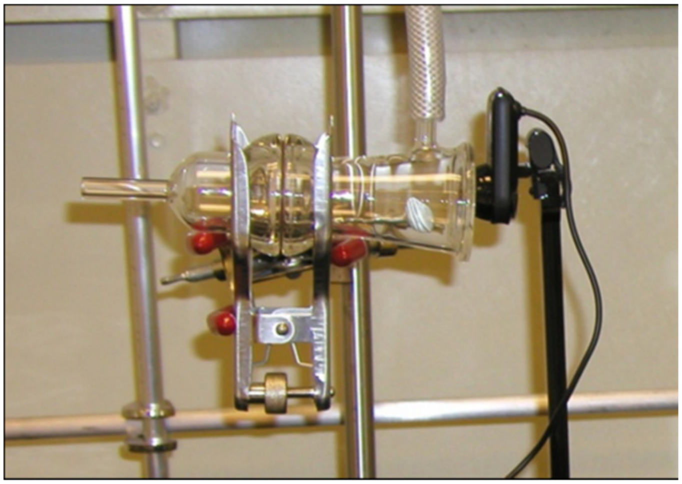
Figure 10. Colorimetric indicator testing chamber

Relative humidity was produced by a Perma Pure fuel cell humidifier sized to humidify air at rates up to 150 slpm. A Julabo MC-12 circulating bath supplied the humidity module with a continuous flow of temperature-controlled, distilled water to use during the production of humidity.


Figure 12. Before (left) and after (right) photos from basic vapor testing in TDA's first colorimetric indicator testing apparatus

Streams of dry air, humid air, and air contaminated with the chosen TICs were mixed and sent through a flat-plate heat exchanger to produce a temperature-controlled stream of air with the appropriate TIC challenge concentration. The temperature-controlled air stream was delivered through insulated lines to the indicator testing chamber where it flowed through, or impinged upon, colorimetric indicator coupons.

Color changes in the colorimetric indicator coupons (Figure 12) were monitored and recorded by a webcam, shown in Figure 10, connected to a laptop computer.

At the end of the Phase I project, the apparatus was adapted to test our first ESLI-enabled, carbon bed, filter cartridges. The transparent filter housings were produced by MSA.


Figure 11. Prototype testing with the first ESLI apparatus

Testing the first ESLI-enabled, carbon bed, filter cartridges with the Phase 1 apparatus (Figure 11), and the challenges that the testing presented, helped to define the requirements for the Phase II vapor test apparatus.

2.1.4.2.2 Design and operation of the Phase II vapor test apparatus

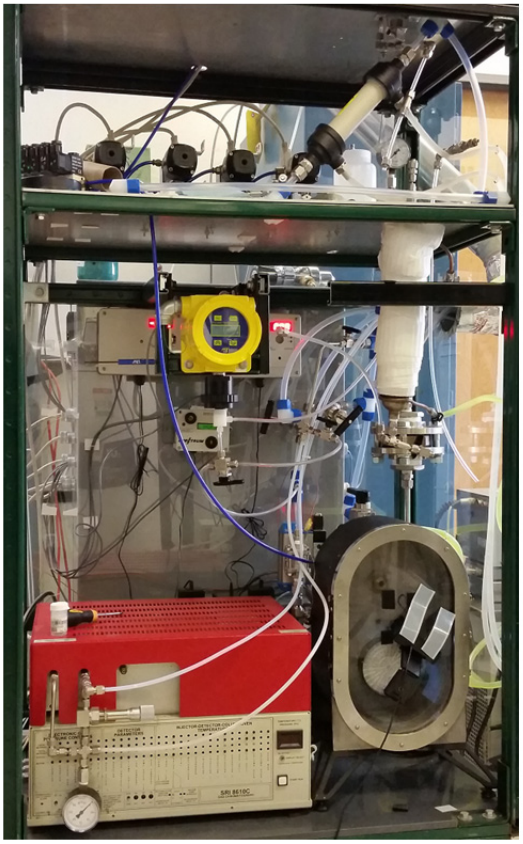

Figure 13. Phase II vapor test apparatus

The vapor test apparatus that we built to test filter cartridge prototypes during the Phase II was an automated filter testing system. One of TDA's OPTO 22 PAC control systems was customized to control the apparatus components' variable functions.

Air flows were set by the apparatus operator and controlled by MFCs. Acidic and basic vapor concentration readings from Gas Sensing's D-12 gas transmitter were logged by the OPTO 22 system. VOC vapor concentrations were analyzed by GC or FTIR and logged by the control system. The temperatures of the filter cartridge testing chamber, relative humidity module, and the solvent bubbler were set by the apparatus operator and were controlled by the Julabo recirculating baths' control systems.

Still photos from the Logitech webcam were captured by WebCamImageSave (a freeware WebCam capture utility). The photos were timestamped by the computer's operating system during the save operations, which allowed them to be correlated with TIC concentration data during post-test processing.

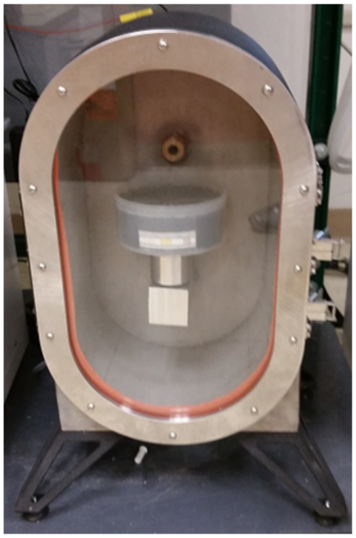

Figure 14. Filter testing chamber

L a b color differences (ΔE_{ab} , see Appendix I in section 2.1.6 for a description of ΔE_{ab}) between the colorimetric indicators and their reference color strips were calculated during post-test processing of the WebCam's photos. The L a b color difference calculations were performed by a Python program written by TDA's David Eisenberg to automate the post-test image processing.

The filter cartridge testing chamber, see Figure 14, is the key component in the Phase II vapor test apparatus. It was constructed from stainless steel to improve its corrosion resistance to acidic and basic challenge gases. The filter cartridge testing chamber is a jacketed enclosure that uses a recirculating bath to control the enclosure's temperature and the temperature of the challenge gas stream that flows through it. Once the challenge gas stream arrives at the testing chamber, it travels 15 linear feet through a ½" OD tube that wraps around the inner wall of the racetrack-shaped testing chamber five times. The 5-circuit, ovalized, 15-foot path provides adequate mixing and residence time to produce an isothermal gas stream as it exits into the chamber's internal volume. The challenge gas stream enters the chamber's test space parallel to the testing chamber's inner surface on the upper right corner of the chamber where the upper cylindrical surface begins, which creates swirling, counterclockwise flows (from the chamber window's point of view). The challenge gas stream is pushed through the filter cartridge and exits the testing chamber heading for either the gas transmitter, for acidic or basic gases, or to the GC/FTIR for VOC vapor analyses.

2.1.4.2.3 Indicator sensitivity testing

The intensity and contrast of the color change produced by a given contaminant concentration in a given time is determined by the reactivity that we achieve during indicator formulation. Thus, we conducted a series of experiments where we measured the intensity of the color change as a function of contaminant concentration at or below the test contaminant's permissible exposure limit (PEL). The reactivity of each indicator formulation was evaluated by measuring the magnitude of its color change. Color change intensities of the indicators were measured spectrophotometrically before and after exposure to vapors and the color change (ΔE_{ab}) was subsequently quantified using the CIE L a b color system (for a description of the CIE L a b color system, see Appendix I). Though color changes as low as ΔE_{ab} =2.3 can be detected by the human eye (Fraser, 2004), changes of $\Delta E_{ab} \geq 10$ are recognized as being easily seen, therefore we used an ΔE_{ab} of 10 as our lower limit for an acceptable color change.

For these tests, after an initial color measurement, each indicator was exposed to an appropriate test vapor (acid, base, or OV) at 10%, 50% or 90% of the gas's PEL for 15 minutes; at that time, the test was ended and the color was re-measured. Gas flow rates past the indicators were kept constant at 64 L/min. Additionally, temperature and relative humidity (RH) were varied to determine their effect on the color changes of the indicators. At each vapor concentration, 3 different temperatures (-10, 20, and 40°C) and 3 different RHs (5, 50, and 95%) were evaluated, resulting in a total of 27 tests for each indicator formulation (81 total tests for the three indicators). Under each test condition, the indicator color change (ΔEab) was calculated.

Due the large number of test conditions and results for each indicator, the data set was analyzed statistically using a 33 factorial design (i.e., 33 = 27 experiments; 3 indicators with 3 variables each) in order to determine the effects of RH, vapor temperature and vapor concentration on our ESLI indicators for SO2, NH3 and isopropyl alcohol (IPA). In a full-factorial experimental design, each variable is tested at a low, intermediate and high value, and the responses are measured in each of the individual experiments (Box, 1978). The measured response was the color change of the indicator (ΔEab - see

Appendix I). The resulting data allowed us to determine the effect of each variable on the performance of the indicators and thus evaluate the indicators' reactivities (i.e., magnitude of the color change) under various environmental conditions.

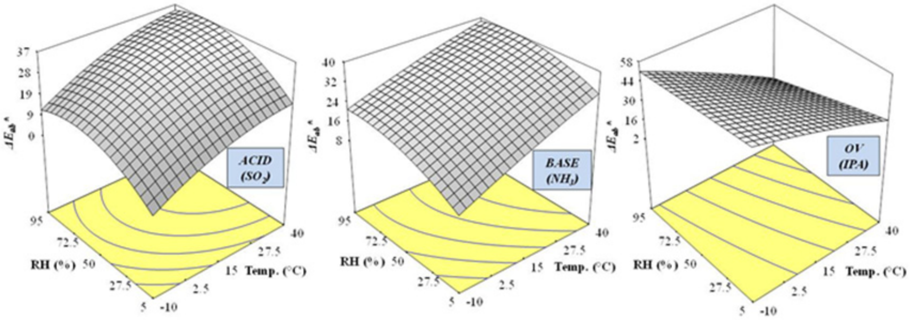

Figure 15. Response surfaces (generated from a 33 full factorial design analysis of the experimental data) showing the effect of RH and temperature on the three indicators' color change responses when exposed to test vapors

Figure 15 shows the response surfaces from the factorial analysis that show how temperature and RH affected the color change (the ΔEab response) of the various indicators. Not surprisingly, the acid and base indicators, which behaved similarly in all tests, exhibited greater color change with increasing RH (which increases the H2O concentration) and increasing temperature (which increases the reaction rate) as shown by the upward slope of the corresponding response surfaces in Figure 15. Importantly, the greatest response occurred when RH and temperature were simultaneously increased (indicating an interaction between these variables); this interaction effect could easily be missed without the use of the factorial analysis. Additionally, as expected, the color change response also improved as the acid or base test vapor concentration was increased (response surfaces not shown); the greatest color change was effected when all three increased simultaneously. In contrast, the response of the OV indicator to IPA under various conditions was different to that observed for the acid and base indicators, as clearly shown by the downward slope of the OV response surface in Figure 15. As with the acid and base indicators, the response of the OV indicator in the ESLI increased with IPA concentration (data not shown); however, most surprisingly, increasing the temperature and RH decreased the response of the OV indicator. The reasons for this are not clear. It is clear, however, that the OV response surface further emphasizes the complicated effect that water has on the OV indicator, with water being required for the color-change reaction, but also hindering the OV-indicator interaction with organics.

Based on this data analysis, when using the criteria of ΔEab ≥10 as a visible color change, the indicators were observed to visually detect the test vapor in all cases, with the exception of ammonia at the very lowest humidity and concentration (5% RH, -10°C, and 5 ppm NH3), consistent with the results predicted by the factorial analysis. It is important to note that the criteria used for these tests included a test time limit of 15 minutes, thus a ΔEab ≥10 does not necessarily indicate that an indicator cannot be used under the conditions tested, but that we simply need to further refine our formulation or increase the time required to view the color change to a period >15 minutes. The sensitivity of the indicators was determined to be appropriate for use in the ESLI modules.

Table 2. Times needed to achieve a ΔEab ≥20 for OVs at their PEL

VOC	P.E.L. (ppm)	time for color change at P.E.L.
IPA	400	< 10 minutes
Toluene	200	< 60 minutes
Ethanol	1000	< 25 minutes
Acetone	1000	< 75 minutes
DCM	25	< 45 minutes
Cyclohexane	80	< 45 minutes
Pentane	1000	< 15 minutes
Xylene	100	< 30 minutes

TDA also tested the OVs shown in Table 2. These additional analytes, though not tested to the extent required for the factorial design, were tested under conservative, challenging conditions for our OV indicator as predicted by the results of the factorial design (i.e., humid conditions, room temperature). The OVs were tested at their PEL, 20°C, and 50% RH to determine the time required for a complete indicator color change (gas flow = 4 L/min). Table 2 shows the time it took for the color change to occur; in all cases, the color changes had ΔEab 20-30 (much greater than needed to be easily visible, 10 is visible). Though many gases, especially the more hydrophobic gases, required a longer indicator response time, each indicator changed color in a small fraction of the typical 8-hour cartridge life.

2.1.4.3 False positive and interference testing

Carbon dioxide (CO_2) in the atmosphere is approximately 0.04% by volume, and as such is not expected to interfere with the function of our ESLI. In certain industrial environments, however, elevated levels of CO_2 may cause false positive readings for the acid indicator since water vapor and carbon dioxide (CO_2) form carbonic acid. For this reason, we tested the stability of our acid indicator materials in the presence of high levels of CO_2 and humidity. The occurrence of false positives by elevated CO_2 levels was tested for both aerosols of carbonic acid, produced by bubbling 100% CO_2 through a water aspirator, as well as formation of carbonic acid in the vapor phase by passing a pure CO_2 gas stream over a humidifying Nafion® membrane. In both cases, after 8 hours of constant exposure to a humidified CO_2 gas stream, only a slight fading of the purple acid indicator color was observed; at no time did the acid indicator fully switch from purple to gray, as is normal for the acid indicator on exposure to acid. A comparison of the acid indicator strips before and after the carbonic acid exposure tests is shown in Figure 16. We concluded that the formation of carbonic acid from CO_2 and humidity would not cause our acid indicators to produce false positive readings since there would rarely be a storage or work environment that would be even 1/10th as concentrated as the one endured by the indicators during false positive testing.

Figure 16. A new, unused acid indicator strip (left) compared to the used indicator strip (right) tested at 100% RH in a CO_2 gas stream for 7 hours. Though the purple color faded during the 7-hour exposure, a color change (to gray) was NOT observed.

2.1.4.4 ESLI lifetime/shelf-life determination

In Task 4, we performed tests to determine the shelf-life of the ESLI indicator formulations. The goal was to develop formulations with the appropriate shelf-lives and activities that would be needed in a commercial ESLI module. Using the indicator materials prepared in Task 1, TDA performed shelf life determination under normal storage conditions (20-25 °C at 23-30% RH); the indicators were stored in common polyethylene plastic bags. The indicators stored under these conditions showed no degradation, color change or inactivity following two months of aging. Furthermore, the indicators stored under these conditions showed a rapid response when exposed to test vapors from the appropriate class. After six months of aging in plastic bags the indicators began to lose reactivity and after eight months, which occurred in February, they were non-reactive. Winter RH levels inside heated buildings in Colorado can drop below 10%. We learned that storage in vessels that permit H_2O to exchange with the local atmosphere can lead to the indicators over drying. In addition to the tests described above, we explored other variables that might affect the aging and shelf life of the indicator materials, such as exposure to sunlight.

Photodecomposition of the ESLI indicators was studied by exposing samples to the controlled radiation produced from a Newport Corporation Oriel, Model Sol1A, Class ABB Solar Simulator. This instrument employs a xenon lamp and appropriate filters to simulate solar radiation and is factory certified to meet the ASTM E 927-05 standard of 1 sun output, approximating a standard noon-time sun. For reference, a solar spectrum, to which ESLIs might be exposed if used in direct sunlight, or in diffuse daylight, is shown in Figure 5.

It was verified that the permanganate ion and bromocresol purple were both highly photosensitive and faded rapidly upon exposure to simulated daylight. The brilliant-yellow fared much better, retaining 87.5% of its yellow color intensity on Whatman Filter Paper #4 after 4-hours of 800 W exposure.

Color changes (fading) were quantified using a BYK-Gardner Model 6850 Color-Guide Plus 45°/0°-11 mm instrument, which was calibrated using a white, black and green color standard (BYK-Gardner Standards, 6811, 6810 and 6812, respectively).

Within two hours of exposure to simulated solar radiation at 800 W, samples of both sodium permanganate and bromocresol purple were bleached. The samples supported on γ-alumina and Whatman Filter Paper #4, respectively, became very light in appearance. The results verified the Phase I observations that color faded upon exposure to light and implied that long-term storage (2-3 years) will be an issue if these indicators are not protected from solar and artificial sources of radiation before use.

A portion of the V3 ESLI-enabled filter cartridge prototypes underwent a durability conditioning protocol that the U.S. military uses to test CBRN filter cartridges. Fourteen of the V3 ESLI-enabled filter cartridge prototypes began the protocol detailed in Table 3 below. Four cartridges, Group 1, were withdrawn for testing after the hot diurnal test.

Table 3. A durability conditioning protocol used by the U.S. military to test CBRN cartridges and the effects of the protocol on the V3 prototype's indicators

Test	Test Method	Test Condition	Duration
Hot Diurnal	Mil-Std-810F; Method 501.4; Table 501.4-II; Hot-Induced Conditions	Diurnal Cycle, 35° C (95° F) to 71° C (160° F)	3 Weeks
Cold Constant	Mil-Std-801F, Method 502.4;	Basic Cold (C1), -32° C -25.6° F); Constant	72 Hours
Humidity	Mil-Std-810E, 507.3; Method 507.3; Table 507.3-II	Natural Cycle, Cycle 1, Diurnal Cycle, 31° C (88°F) RH 88% to 41° C (105° F) RH 59%	5 Days, Quick Look
Group 1	Hot Diurnal only	Acidic: Color OK, no reactivity Basic: Color OK, Reactivity good VOC: Color change	A: Fail B: Pass V: Fail
Group 2	Hot Diurnal & Cold Constant only	Acidic: Color OK, no reactivity Basic: Color OK, Reactivity good VOC: Color change	A: Fail B: Pass V: Fail
Group 3	Hot Diurnal, Cold Constant, and Humidity	Acidic: Color OK, no reactivity Basic: Color OK, Reactivity good VOC: Color change	A: Fail B: Pass V: Fail

Four cartridges, Group 2, were withdrawn for testing after the cold constant test. The six remaining V3 ESLI-enabled filter cartridge prototypes, Group 3, underwent the entire durability conditioning protocol.

The Group 1 through 3 rows in Table 3 report the efficacy of the group's indicators after their various levels of conditioning. Only the basic vapor ESLI indicators survived the three week exposure to the hot diurnal cycles. The basic vapor ESLI indicators survived the entire protocol without a loss of reactivity. It is unknown whether the acidic and VOC indicators would have survived the other two segments of the durability conditioning protocol without a loss of reactivity if they had not been exposed to the 71° C daytime temperatures of the hot diurnal cycles.

It is known that temperatures above ~50°C lead to decomposition of $NaHCO_3$, to the much more basic Na_2CO_3, which leads to decomposition of permanganate. Failure of the VOC indicators to survive the hot diurnal cycles was an unfortunate if not expected result.

The acidic indicators' pH sensitive dye, bromocresol purple, decomposed into a purple product that had no pH sensitivity during the hot diurnal cycles. The decomposition mechanism is unknown at this time.

2.1.4.5 Prototype design and fabrication

The goal of Task 5 was to develop ESLI-enabled filter cartridges to the point that they were ready for testing and certification by the NPPTL at NIOSH.

2.1.4.5.1 Prototype designs

2.1.4.5.1.1 Design of the first ESLI-enabled filter cartridge prototype

The purpose of TDA's first, ESLI-enabled filter cartridge (the V1 prototype, Figure 17) was to demonstrate that the colorimetric ESLI indicators would operate as intended when they were installed inside carbon-bed filter cartridges. A successful demonstration of end-of-service-life-indication by the V1 prototypes hinged on two factors, the first was TDA's ability to create an air stream inside the filter cartridge that would cover the viewable surfaces the colorimetric indicators. The second factor in the successful demonstration of the V1 prototype's ESLI capability was that any design had to maximize the visual accessibility to the colorimetric indicators without disrupting the airstream that covered the indicators.

We provided a slipstream path, for the portion of the carbon bed's fully developed flow that intersected the ESLI strip, in order to create a small air stream that would enrobe the ESLI indicators. The slipstream path was created by providing an air flow path that was less restrictive (lower in pressure drop) than the carbon bed's. The slipstream passed through one layer of polypropylene felt, flowed over the ESLI indicators, and re-entered the carbon bed through another section of polypropylene felt. Precisely dimensioned spacers were used to position the colorimetric ESLI indicators close enough to the translucent filter housing's inner wall that they were visible, yet far enough away from the wall to avoid disrupting the air stream that was forced to flow between the viewable surface of the ESLI indicators and the translucent filter housing's inner wall.

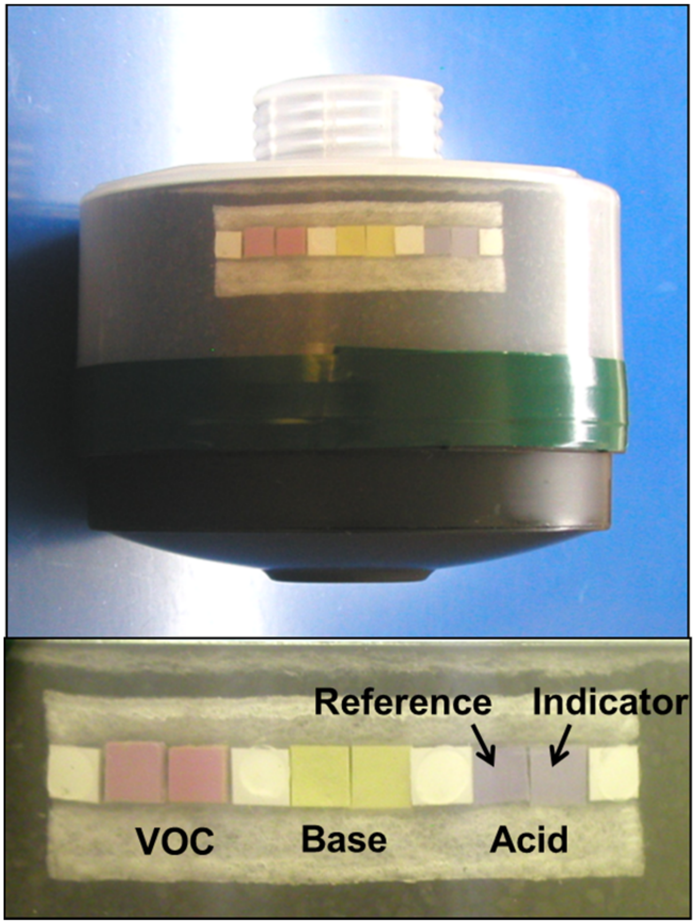

Figure 17. The first ESLI-enabled filter cartridge prototype

The translucent filter housings supplied to TDA by MSA exhibited a optical characteristic known as contact clarity. Contact clarity is a term used in multiple industries that signifies the ability to view objects through a translucent membrane when the objects are in contact with said membrane. The downside to contact clarity is that as the separation distance from the translucent membrane to the objects increases, their transmitted images become less distinct, until they are not visible at all. Frosted glass is an excellent example of a translucent material that exhibits contact clarity.

The V1 ESLI-enabled filter cartridge prototype's indicators were designed to be mounted to the filter housing so that their downstream edges were 70% of the way through the carbon bed's depth. This position was designed to ensure that the slipstream would re-enter the carbon bed with at least 20% of the bed's depth remaining, protecting the user from any TICs that might be in the slipstream.

2.1.4.5.1.2 Design of the ESLI-enabled filter cartridge prototype V2

By the time we began designing the V2 ESLI-enabled filter cartridge prototypes we had discovered that the indicators would not survive long term storage with most carbon beds. We identified two major issues in the V1 ESLI-enabled filter cartridge's design:

1. Users were unable to see the ESLI indicators on their filter cartridges
2. The ESLI indicators were always in vapor contact with the carbon bed

The V2 prototypes featured snap-in ESLI modules, shown in Figure 18, that were stored in heat sealed, metalized pouches that were designed to be torn open and inserted into

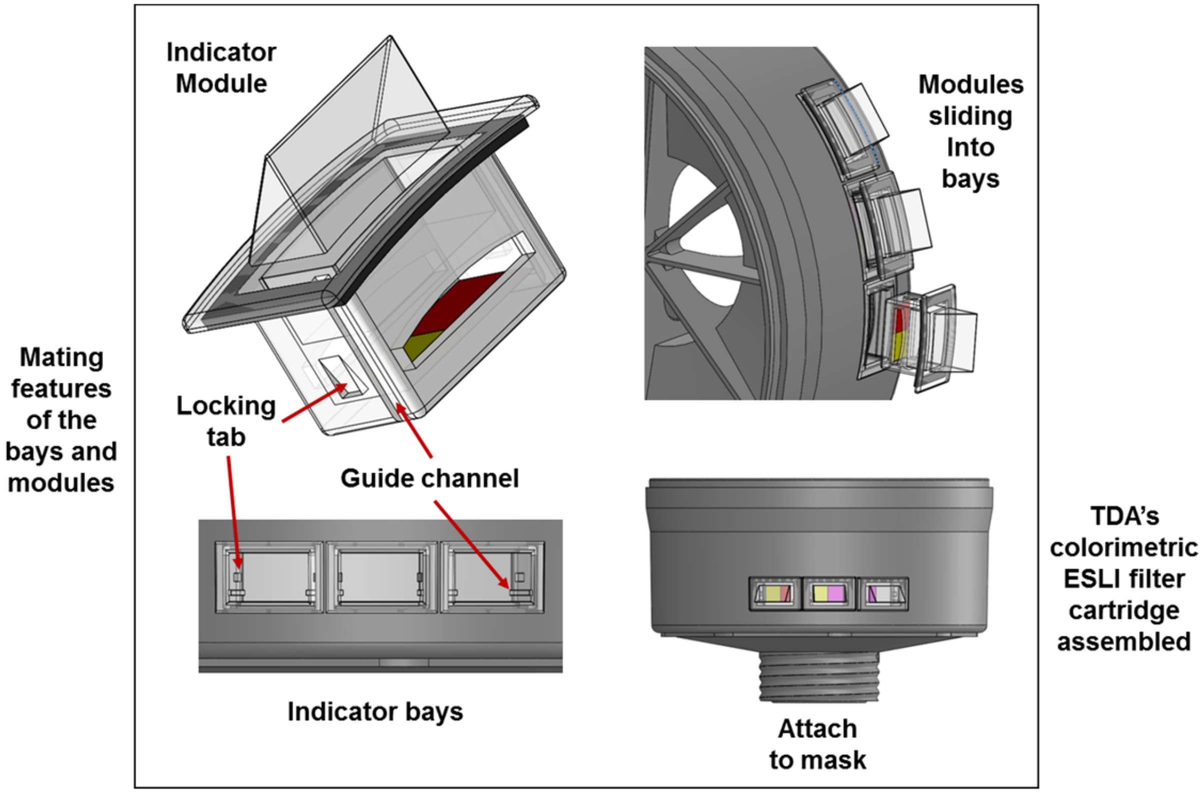

Figure 18. Design of the V2 ESLI-enabled filter cartridge prototypes

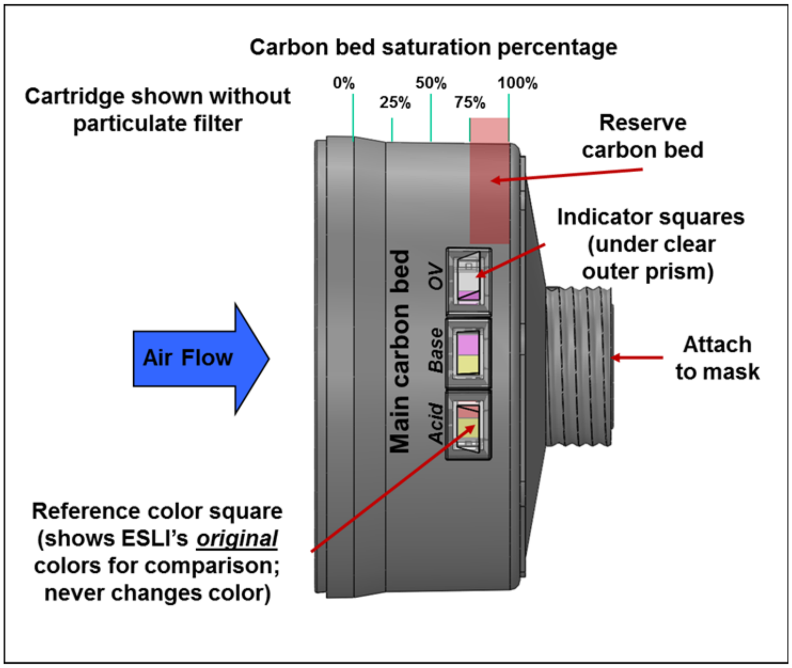

Figure 19. Graphical explanation of the reserve carbon bed in the V2 ESLI-enabled filter cartridges

the filter cartridge when it was about to be used. The ESLI modules featured soft, silicone gaskets that sealed against the ESLI module bays' outer flanges to eliminate any leakage of air through the sealing surfaces.

The V2 prototype's ESLI modules were designed to place the colorimetric indicators in the slipstream when they were inserted into the filter cartridge. Color changes from the ESLI indicators could be monitored by the user through prisms that both illuminated the subsurface ESLI indicators with ambient light and transmitted reflected images of the ESLI indicators to the user.

The V2 prototypes were produced in two configurations: one with three ESLI modules per filter cartridge, and one with one ESLI module per cartridge. The two configuration were identical in their operation other than the number of ESLI modules that a user would need to snap into them.

The V2 ESLI-enabled filter cartridge prototypes were designed to have either one or three ESLI module bays molded into their filter cartridge housings. The ESLI module bays were designed to mate perfectly with the snap-in ESLI modules. The mating features (tongue and groove type) prevented improper ESLI

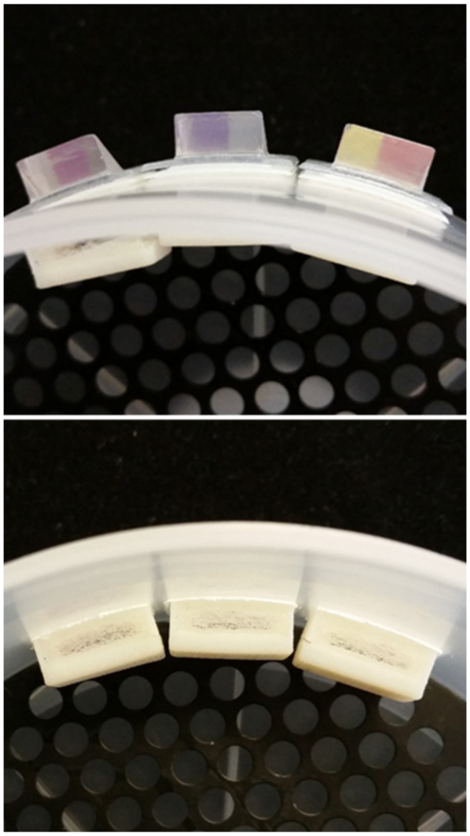

Figure 20. V2 prisms and bays

module insertion, ensuring that the prisms would always face the user after insertion.

Similar to the V1 ESLI-enabled filter cartridge prototype, the V2's indicators were designed to be inserted into the filter housing so that their downstream edges were 80% of the way through the carbon bed's depth, see Figure 19. This position was designed to ensure that the slipstreaming air stream would re-enter the carbon bed with at least 20% of the bed's depth remaining, protecting the user from any TICs that were in the slipstreaming air stream while the ESLI indicators were changing color.

Figure 20 shows photos of the V2's prisms reflecting color changes and of the ESLI module bays mounted in a V2 filter cartridge. Randomly oriented polyester scrim was used to keep carbon from entering the ESLI bays. The V2's ESLI bay design extended further into the carbon bed and had well defined inlets and outlets normal to the slipstream that triggered color changes in the ESLI indicators.

The V2 prototypes underwent several redesigns to their prisms, over the course of a year, before it was determined that they were not reliable enough in their ability to light the internally mounted ESLI indicators or to reflect easy-to-see images of the changing ESLI indicators to be considered commercially viable.

2.1.4.5.1.3 Design of the ESLI-enabled filter cartridge prototype V3

Our successes at creating the slipstreams that were used to produce ESLI indicator color changes in the V1 and V2 prototypes led to the design for the V3 ESLI-enabled filter cartridge prototypes.

The V3's design addressed both the lighting and image reflection issues of the V2 prototypes by moving the colorimetric ESLI indicators onto the outside of the filter cartridges, see Figure 21.

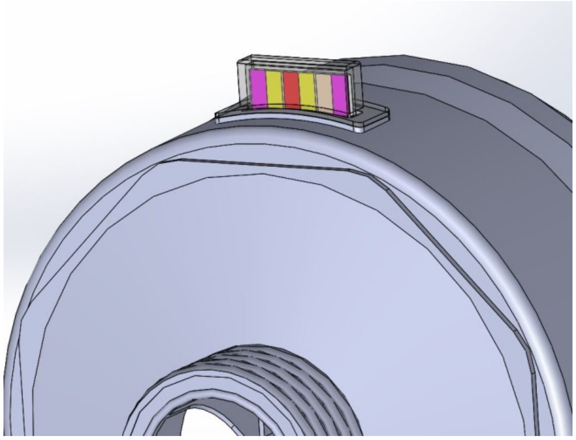

Figure 21. The externally mounted ESLI indicators of the V3 prototypes

The V3's ESLI modules were still stored in heat sealed, metalized pouches prior to use to protect them from TICs in the environment during storage and they snapped into the filter cartridge housings in the same way as the V2's ESLI modules. They used integrated, silicone gaskets that were over molded onto the snap-in ESLI modules. The soft silicone gaskets stopped gas leakage at the mating surface between the ESLI modules and the filter cartridge housings.

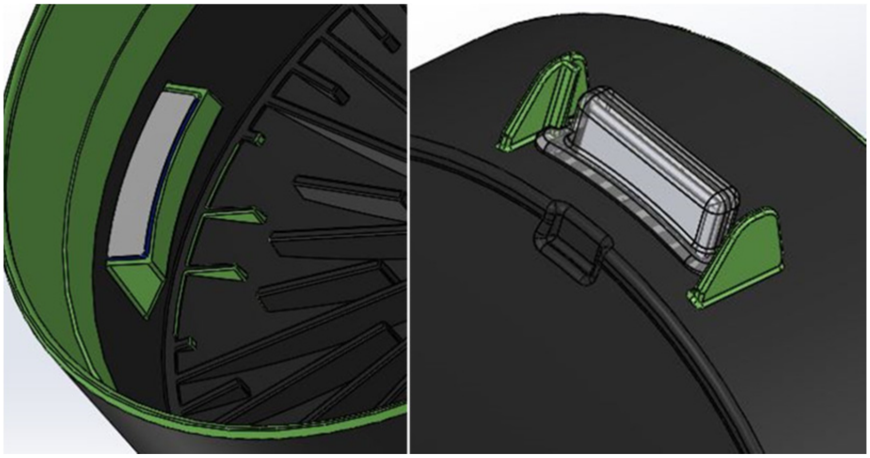

Figure 22. Final models of the V3's internal and external features

The inlet from the carbon bed to the ESLI modules' slipstream is normal to the fully developed air flow in the carbon bed, as shown in the left panel of Figure 22. However, the V3 ESLI module's outlet that returns the slipstream back to the carbon bed is angled to help ensure proper carbon compaction under the ESLI module's intrusion into the carbon bed.

The flow path description below describes the slipstream's path as it moves from left to right in Figure 23.

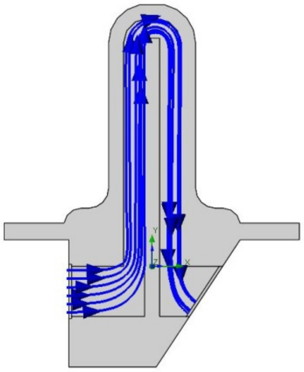

Figure 23. A cut-plot showing the slipstream's path in the V3 ESLI module

The slipstream that triggers the V3 ESLI indicators' color changes enters through the inlet on the ESLI module's intrusion into the carbon bed, see the left panel of Figure 22, and turns 90° towards the clear ESLI module. The slipstream flows along the back of the ESLI indicator tab (the side that faces away from the filter cartridge user) until it reaches the end of the clear ESLI module where it changes direction by 180° around the end of the ESLI indicator tab to flow back over the ESLI indicators and return to the carbon bed. Vapor testing has proven that the V3 prototype's longer slipstream path didn't impact the ESLI indicators' color change rates; they were the same as the V1 and V2 prototypes color change rates.

2.1.4.5.2 Prototype fabrication

The following subsections detail how the three versions of prototypes were constructed.

2.1.4.5.2.1 Fabricating the first ESLI-enabled filter cartridge prototype

We assembled the first respirator cartridge prototype with our V1 ESLI strip (lower panel of Figure 17, page 28). The V1 prototype used a transparent filter cartridge body, specially fabricated by MSA for our tests, and one each of the three indicator pairs developed for the V1 prototype. The V1 ESLI strip was attached to the inner wall of the clear filter housing by thermally welding the ESLI strip's polypropylene felt to the plastic filter housing. The V1 prototype was then filled with an activated carbon that is used in commercial cartridges, which MSA supplied. Figure 17 also shows the assembled cartridge.

Each indicator consisted of a pair of color-matched blocks - the indicator block and a reference block. The reference block, placed right next to the indicator, does not change color; it was just a printed square whose color matched the color of the unreacted indicator. The reference block provides a convenient and quick method for the user to determine by comparison if a color change has occurred.

2.1.4.5.2.2 Fabricating the V2 ESLI-enabled filter cartridge prototype

The V2 ESLI-enabled filter cartridge prototype's smaller components, shown in Figure 18 on page 29, were fabricated by 3D System's Quickparts service. The filter cartridge housings were supplied by MSA and were modified by hand to accept the ESLI module bays. The module bays were fitted with polyester, randomly-oriented, scrim sheet screens to keep carbon from entering the module bays after the filter cartridges were filled with carbon. The ESLI module bays were then epoxied into the filter cartridge housings. After the filter cartridge assemblies were fully cured, they were filled with carbon and the aluminum retention plates, supplied by MSA, were pressed into the filter cartridge housings to maintain carbon compaction.

To decrease the time for challenge gases to break through the carbon that was upstream from the ESLI module's inlet port, later cartridges were only partially filled with carbon (to just above the ESLI module's inlet port) before a scrim sheet was laid down to separate the dissimilar media and the rest of the filter cartridge was filled with soda lime glass beads. The partially inert, two-layer filling method had the effect of producing rapid break through to the 70% level before the remaining 30% of the bed began absorbing the challenge gas' TICs as a commercial carbon bed filter cartridge would. Color changes normally occurred in the first few hours of the test, whereas it was usually ten to twenty hours before challenge gases broke through the remaining 30% of the carbon beds. In many cases the tests were halted prior to carbon saturation to save the bottled challenge gases.

The V2 single-pair ESLI modules (three modules per filter cartridge) had six components. The components of the V2 single pair ESLI modules were the prism, the module body, the silicone gasket, glue (either super glue or VOC-free glue depending on the module type), a reference color block, and an indicator block.

Assembly of a single pair ESLI module began with gluing the reference and indicator blocks to the surface at the bottom of the module body. Then the prism cap was glued to the module body and the silicone gasket was slipped over the module body and glued to the flange surface on the prism cap that mated to the module bay's flange on the filter cartridge. Assembly of the single pair ESLI module was complete at that point.

The V2 three pair ESLI module's assembly process was essentially the same as a single pair module's assembly process. There was a waiting period after gluing the acidic and basic indicator blocks into the module body that allowed the VOCs from the glue to completely evaporate before assembly proceeded to the VOC indicator block's addition to the array of indicators in the bottom of the module body. From that point assembly was identical to the single pair module's process.

2.1.4.5.2.3 Fabricating the V3 ESLI-enabled filter cartridge prototype

The V3 ESLI-enabled filter cartridge prototype's plastic components were injection molded for TDA by Exact Engineering Inc., Holland, MI.

The ESLI module's clear covers and the ESLI indicator tabs were delivered to TDA for assembly into active V3 ESLI modules. The ESLI indicator tabs were populated with ESLI indicators and their color-matched reference blocks using glue. All the ESLI indicators and their color-matched reference blocks were adhered to the indicator tabs using VOC free glue, then the indicator tabs were allowed to cure overnight. After drying, the ESLI indicator tab assemblies were snapped into position in the clear ESLI module covers. The V3 ESLI module assembly process was complete at that point. The ESLI modules were individually heat sealed into metalized bags for storage.

At AVON, in Cadillac, MI, the injection molded V3 filter cartridge housings were loaded with baseplates (the lower carbon support), and scrim inserts (small parts that keep carbon from entering the ESLI module port on the filter cartridges) and then the carbon was drop-filled into the filter cartridges. The upper carbon compression plates, called grids, were glued in place with polyurethane to attach them to the filter cartridge housings' inner walls. HEPA filters were inserted into the filter cartridge housings on top of the grids and they were spin-bonded to the filter cartridge housings using PU to fill and seal their edge gaps. Lids were thermally welded to the filter cartridge assemblies and the assembly process was complete.

The V3 filter cartridges were paired with ESLI modules in their heat-sealed, metalized bags. Together, they were heat sealed into AVON's plastic shipping canisters. Fourteen of the sealed shipping canisters were placed into the U.S. military's Mil-Std-810F CBRN respirator durability conditioning protocol in AVON's environmental chamber. The remainder of the 30 filter production run was shipped from AVON to TDA's Table Mountain facility in Golden, CO for testing.

2.1.4.6 Prototype testing

Three different prototype designs were vapor tested in Task 6. The bulk of the ESLI indicator sensitivity data were collected during the Task 6 testing.

2.1.4.6.1 Acidic vapor testing

Figure 24 shows an exemplar acidic vapor test. SO_2 and HCl vapor tests were run at 4.5, 2.5, and 0.5 ppm, which represent 90%, 50%, and 10% of their OSHA PELs.

The red trace's peak at the beginning of the test, shown in Figure 24, was a quick check to make sure SO_2 was present in the challenge gas before the challenge gas was routed into the filter testing chamber. The challenge gas did not break through the 20% reserve carbon bed during the 11.2 hour test. The acidic vapor tests were run until the acidic vapor ESLI indicators' ΔE_{ab} 's stopped changing.

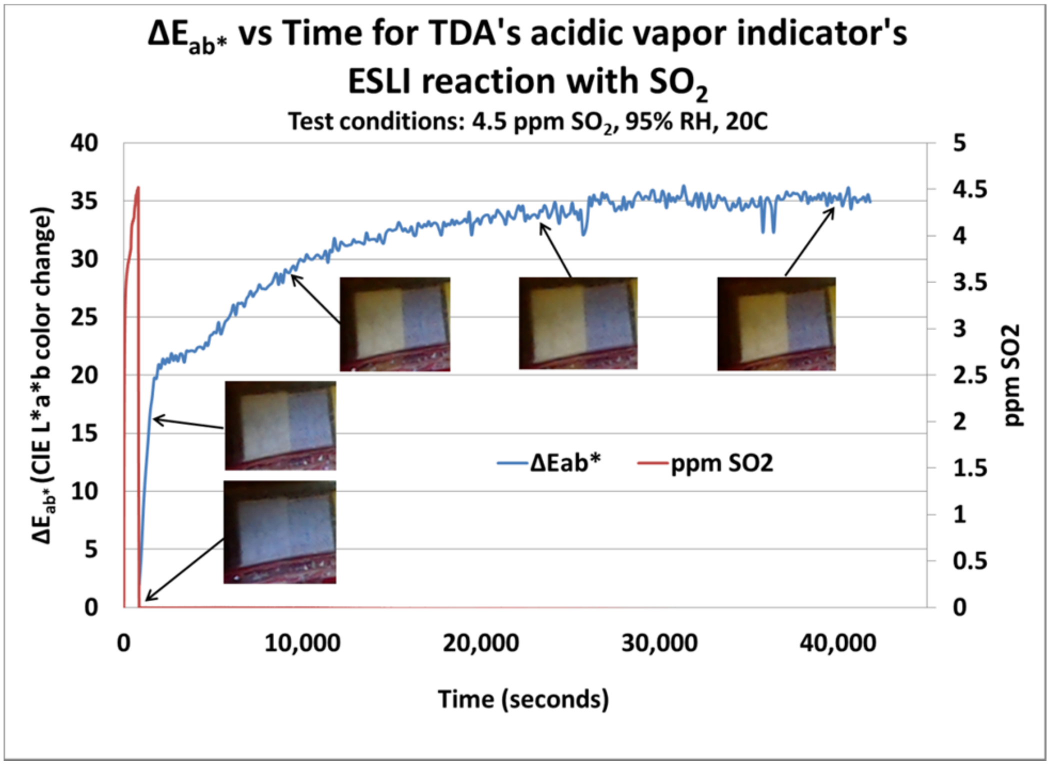

Figure 24. Plot of ΔE_{ab} vs. time for an acidic ESLI indicator exposed to 4.5 ppmv SO_2

The acidic TICs were supplied from compressed gas bottles. SO_2 was delivered by a 200 ppm SO_2 in N_2 bottle. Flows from the acidic gas bottles were diluted to challenge gas concentrations with varying amounts of dry and humidified breathing air as required for a given test.

2.1.4.6.2 Basic vapor testing

Figure 25 shows an exemplar basic vapor test. NH_3 vapor tests were run at 45, 25, and 5 ppm, which represent 90%, 50%, and 10% of the OSHA PEL for ammonia.

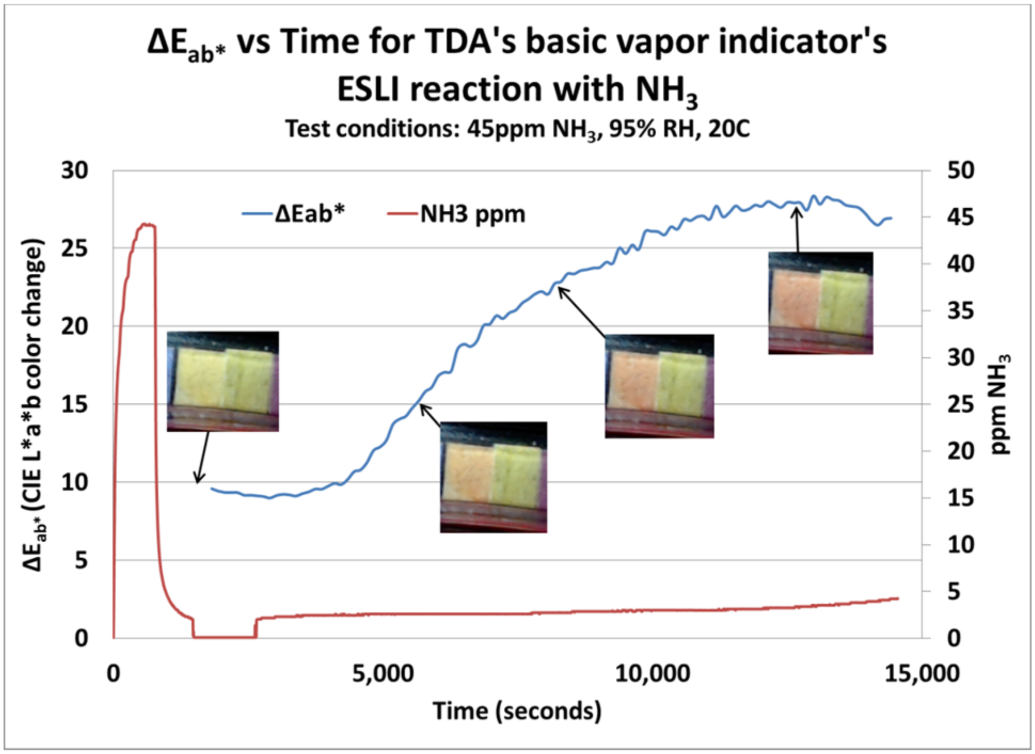

Figure 25. Plot of ΔE_{ab} vs. time for a basic ESLI indicator exposed to 45 ppmv NH_3

The red trace's peak at the beginning of the test shown in Figure 25 was a quick check to make sure NH_3 was present in the challenge gas before the challenge gas was routed into the filter testing chamber. The challenge gas broke through the 20% reserve carbon bed approximately 40 minutes into test. The carbon used in the filter cartridges for the ammonia testing was chosen specifically to permit low concentrations of NH_3 to break through the carbon beds. Early ammonia testing with Molecular Product's Chemsorb 1425, a high-grade, impregnated, activated carbon for the removal of airborne ammonia and amines, led to multi-day tests with no breakthroughs or colorimetric indications. We quickly learned that ammonia can be absorbed or neutralized in large quantities by many different media and we purposefully selected an activated carbon that was not indicated for ammonia removal to keep ammonia vapor test lengths reasonable.

The ammonia gas was supplied from compressed gas bottles. NH_3 was delivered by from 2000 ppm NH_3 in N_2 bottles. Flows from the basic gas bottles were diluted to challenge gas concentrations with varying amounts of dry and humidified breathing air as required for the given test conditions.

2.1.4.6.3 VOC Testing

In this task, the goal was to test the improved permanganate formulations using the measurement techniques previously employed in Phase I, but to expand the list of organic compounds to include: acetone, acetonitrile, benzene, cyclohexane, n-hexane, isopropyl alcohol (IPA), methanol, methyl isobutyl ketone (MIBK), trichloroethylene (TCE) and toluene. Indicator reactivity was tested at relative humidities of 5, 50 and 95%, at temperatures of -10, 20 and 50°C, and at TIC concentrations that were 10, 50 and 90% of their PELs.

Color intensity of the as-produced, permanganated alumina indicators was quantified using a BYK-Gardner Model 6850 Color-Guide Plus 45°/0°-11 mm instrument, which was calibrated using a white, black and green color standard (BYK-Gardner Standards, 6811, 6810 and 6812, respectively). The VOC indicators' measured colors compared favorably to those recorded by the Logitech webcam after adjustments to the lighting system in the vapor test apparatus.

2.1.4.6.3.1 Isopropyl alcohol (IPA)

The first vapor to be tested was isopropyl alcohol (IPA) as recommended by Jay Synder, the lead scientist at NPPTL-TRM (NIOSH National Personal Protection Technology Laboratory-Technology Research Branch. VOC indicators of NaMnO4 + NaHCO3/γ-alumina were exposed to humidified air (95% relative humidity) containing 500 ppmv of IPA, a little over the NIOSH recommended PEL of 400 ppmv. Color change was quantified over a period of hours using the CIE L a b color system and plotting the resulting magnitude of the color change, ΔEab , shown in Figure 26. In the CIE's L a b color system, L is the black-white level; a measures the green-magenta, and b measures the blue-yellow. Here ΔEab , is defined as ΔEab = (ΔL 2 + Δa 2 + Δb 2)1/2. Project goal was to achieve ΔEab s of at least 10, which is a visually apparent color change. The goal was met as indicated in Figure 26.

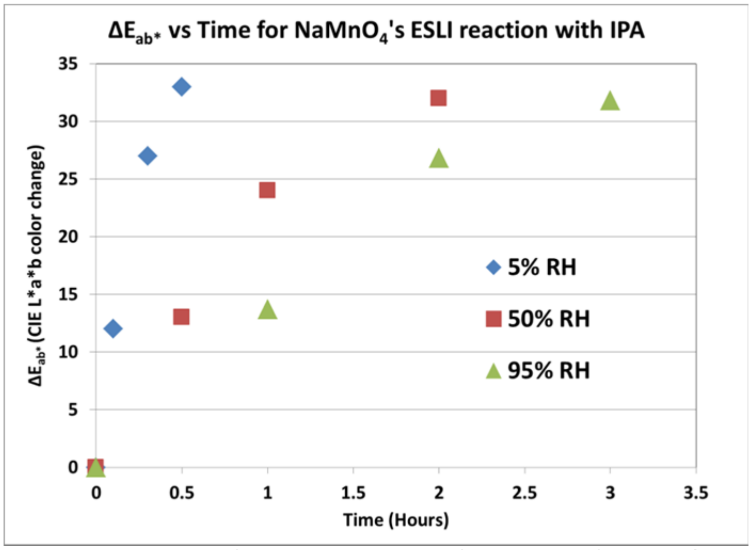

Figure 26. Plot of ΔEab vs. time for pellet of NaMnO4 + NaHCO3/γ-alumina exposed to 500 ppmv isopropyl alcohol for 3 RH levels

Control experiments exposing the indicators to the organic vapors present in the laboratory for 8 h and to humidified air flow for 3 h at 20°C without organic vapors showed negligible color change, and it was concluded that the observed color change was due to oxidation of the isopropyl alcohol. It should be appreciated that the deliquescent $NaMnO_4$ and hygroscopic γ-alumina retain ~20 wt.% water after preparation. This pre-adsorbed water might provide the water necessary for permanganate oxidation reactions in the absence of atmospheric water. Samples tested under lower relative humidity (Figure 26) reacted at a faster rate than those tested under higher humidity. This may imply that the water adsorbed by the highly hydroscopic γ-alumina may competitively block co-adsorption of the organic molecules, or that the smaller pores become flooded at higher humidity levels. It was significant that the indicators functioned well over a wide relative humidity range. Figure 26 also shows results of VOC indicator testing against 500 ppmv isopropyl alcohol in RHs of 5% and 50%. Color change was complete within 30 min and 2h, respectively.

2.1.4.6.3.2 Acetone

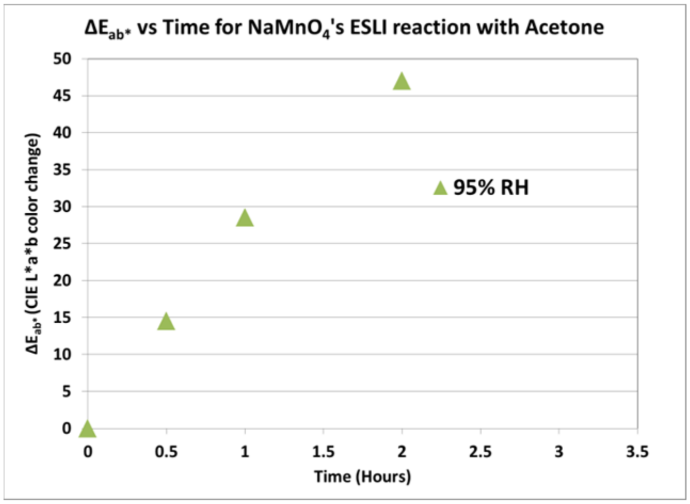

Figure 27. ΔE_{ab} for a VOC indicator of $NaMnO_4$ + $NaHCO_3$/γ-alumina exposed to ~4600 ppmv acetone, air is 95% RH; 20°C

Acetone was evaporated from a bubbler at a rate of 2.9 $g \cdot h^{-1}$. At a molecular weight of 58.08 $g \cdot mol^{-1}$ and 22.414 L/mol (STP), this evaporation rate yields 0.05 $mol \cdot h^{-1}$ or 1.1 $L \cdot h^{-1}$ (STP). This was diluted into humidified air at 20°C flowing at 4 $L \cdot min^{-1}$ = 240 $L \cdot h^{-1}$. This yields: (1.1 $L \cdot h^{-1}$)/(240 $L \cdot h^{-1}$) x 1,000,000 = 4600 ppmv. The NIOSH PEL is 250 ppm. Figure 27 shows results with 4600 ppmv acetone in air of 95% relative humidity and 20°C. Color change was essentially complete within ~2 h. A value of ΔE_{ab} >10, which is deemed necessary for a visible color change, was achieved within 30 min, albeit at very high concentration of acetone.

2.1.4.6.3.3 Methanol

Methanol was evaporated from a bubbler at a rate of 0.531 g/hr. At a molecular weight of 32.042 g/mol and 22.414 L/mol (STP), this evaporation rate yields 0.0166 mol·h-1 or 0.371 L·h-1 (STP). This was bubbled with 50 mL/min and diluted into 3950 mL/min humidified air at 20°C for a total of flowing air of 4 L·min-1 = 240 L·h-1. This yields: (0.371 L·h-1)/(240 L·h-1) x 1,000,000 = ~1550 ppmv. The NIOSH PEL is 250 ppm. Figure 28 shows results of color change with ~1550 ppmv methanol in air at 95% relative humidity and 20°C. Color change was rapid with methanol. A value of ΔEab >10, which is deemed necessary for a visible color change, was achieved within 0.15 h. If linear, 250 ppmv would cause similar color change within 1 h.

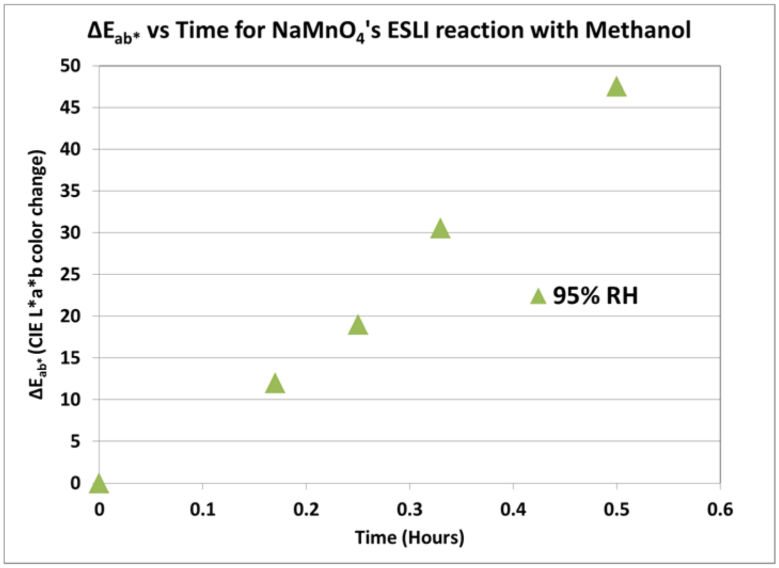

Figure 28. ΔE$_{ab}$ for a VOC indicator of $NaMnO_4$ + $NaHCO_3$/γ-alumina exposed to ~1550 ppmv methanol, air at relative humidity of 95%; 20°C

2.1.4.6.3.4 Toluene

Toluene was evaporated from a bubbler by a dry air flow of 125 sccm. Toluene concentration in the 64 L/min challenge gas flow was confirmed by FTIR to be 100 ppmv. The NIOSH PEL is 200 ppm. Figure 29 shows results of color change with ~100 ppmv methanol in air at 50% relative humidity and 20°C. Color change was rapid with toluene. A value of ΔEab >10, which is deemed necessary for a visible color change, was achieved within 0.5 h.

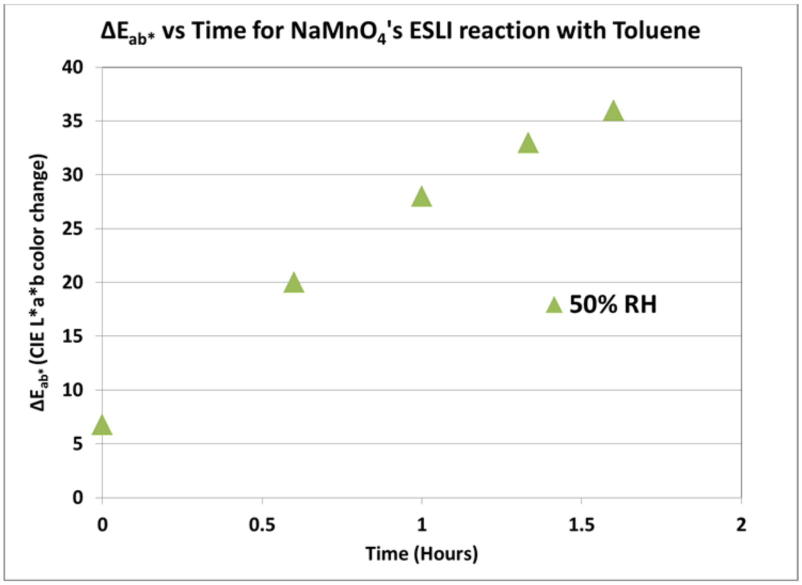

Figure 29. ΔE_{ab} for a VOC indicator of $NaMnO_4$ + $NaHCO_3$/γ-alumina exposed to 100 ppmv toluene, 64 L/min flow rate, air temperature 20°C, RH 50%

2.1.4.6.3.5 Acetonitrile

In these experiments, 2.36 g of acetonitrile was vaporized over a period of 4h into a total of 4LPM of flowing air, 3.95 LPM humidified to 95%. The rate of acetonitrile vaporization is: (2.36 g)(mol/41.05 g)(22.414L/mol)/4h = 0.322 L/h, assuming ideal gas behavior. When this is diluted into a gas stream of air at 4LPM = 240L/h, the concentration of acetonitrile impinging upon the permanganated alumina sample was: ~(0.322 L/h)/240 L/h) x 1,000,000 = ~1340 ppmv. The NIOSH PEL for acetonitrile is 20 ppmv, whereas that for OSHA is 40 ppmv. However, even at these high levels of acetonitrile, which are far in excess of the NIOSH PEL, the ESLI appeared unreactive. In a control, the disks were subsequently exposed to an oxidizable reagent and rapidly changed color, showing that the disks functioned properly and that the acetonitrile did not react.

From the literature, it is well established that acetonitrile readily adsorbs onto γ-alumina at the aluminum Lewis-acid sites. In fact, acetonitrile is often used to titrate the aluminum Lewis-acid sites in various aluminas and in silico-aluminates such as zeolites. Thus, lack of adsorption of acetonitrile onto γ-alumina is not likely the cause of poor reactivity. According to the patent literature (Blackman, Cesa, Attig, U.S. 5,440.068, Aug. 8, 1995), $KMnO_4$ is used to purify acetonitrile of oxidizable organic compounds by refluxing. The colloidal MnO_2 produced by oxidation of the organic impurities is filtered. Alternatively, $KMnO_4$ adsorbed onto γ-alumina has been used to purify acetonitrile of oxidizable organic materials. Moreover, acetonitrile is a solvent of choice for dissolving permanganates, including highly reactive $LiMnO_4$ used to oxidize organic compounds in organic synthesis. In all of the above cases, the acetonitrile is stable and is not readily oxidized by permanganate, even at reflux temperature, although ppmv levels of oxidation are not ruled out. It is concluded that it will be challenging to use $NaMnO_4/\gamma$-alumina in an ESLI to detect acetonitrile unless an additional oxidizing agent or catalyst is added.

2.1.4.6.3.6 Acrylonitrile

Acrylonitrile is oxidized by dilute, alkaline solutions of permanganate, releasing cyanide: $CH_2=CH\text{-}CN + KMnO_4 \rightarrow CH_2=CH\text{-}OH + KCN + MnO_2$. In fact, the oxidation of acrylonitrile by permanganate is used in analytical techniques to quantify acrylonitrile. However, in our attempts to use the permanganated alumina as a colorimetric indicator for acrylonitrile, acrylonitrile appeared unreactive even after 4 h exposure after vaporizing 2.36 g of acrylonitrile, yielding (2.36 g)(mol/53.06 g)(22.414L/mol)/4h = 0.249 L/h. Diluted with 240L/h air at 95% relative humidity, the concentration impinging upon the permanganated alumina sample was: (0.249 L/h)/240 L/h) x 1,000,000 = ~1040 ppmv. However, the PEL for acrylonitrile is exceptionally low: only 1 ppmv according to NIOSH standards and 2 ppmv according to OSHA. The lack of reaction after 4 h exposure to ~1000 times the PEL will be unacceptible for a colorimetric ESLI. However, in the case of acrylonitrile, according to NIOSH, respirators should not be relied upon to protect worker health, in part due to transport through the skin. Instead various engineering aproaches should be used to minimize worker exposure. Quoting from a NIOSH document: “It must be stressed that the use of respirators is the least preferred method of contolling worker exposure and should not normally be used…” . Respirators are recommended in emergency and not for routine, workday use. If this is the case, then colorimetric indicators in respirators should not be considered for acrylonitrile.

The lack of activity of the TDA indicators is attributed to poor adsorption of the acrylonitrile onto the γ-alumina. From the patent literature (Higgins, U.S. 3,262,966, July 26, 1966) γ-alumina is routinely used to purify acrylonitrile. The γ-alumina adsorbs impurities found in acrylonitrile but does not adsorb the acrylonitrile. In addition, γ-alumina is widely used as a catalyst support in the synthesis of acrylonitrile, implying that acrylonitrile is readily desorbed due to weak adsorption on γ-alumina. It is concluded that the failure of the permanganated alumina to change color even after 4h exposure to 1000 ppmv acrylonitrile is due to poor adsorption of acrylonitrile onto the γ-alumina rather than inability of the permanganate to oxidize the acrylonitrile. In principle, the γ-alumina might be modified by addition of Zn or Cu to adsorb the nitrile. However, if NIOSH does not recommend the use of respirators with acrylonitrile, this type of development does not appear justified.

2.1.4.6.4 Oxidation Limitations of Permanganate

TDA tests show that color changes due to chemical reactions are not effective against very chemically stable molecules such as acetonitrile, benzene, trichloroethylene (TCE), etc. The oxidation potential of permanganate ion is 1.679 eV in the reaction: $MnO_4^{-1} + 4H^+ + 3e^{-1} = MnO_2 + 2H_2O$. For many of the refractory organic solvents tested, which are not oxidized by permanganate, it should be noted that organic chemists often dissolve permanganate in such solvents to oxidize other organic compounds that they wish to oxidize. Often these solvents with dissolved permangate are refluxed during such reactions, with the refractory organic solvents remaining essentially inert. $KMnO_4$ is used to purify acetonitrile by oxidizing dissolved organic impurities. If the acetonitrile that was used in the TDA experiments was purified by $KMnO_4$, all volatile impurities that might react with permanganate have been removed, and thus cannot cause a color change. In organic synthesis, acetonitrile is used as a solvent of choice to dissolve permanganates ($KMnO_4$, $LiMnO_4$, etc.), which is used to partially oxidize organic materials. Often, the system is refluxed, with acetonitrile remaining stable. It will be difficult to oxidize acetonitrile using $NaMnO_4$/gamma alumina. There thus appears to be low probability that permanagate alone will be capable of oxidizing the more refractory organic solvents such as acetonitrile, benzene, trichloroethylene, etc. and changing color.

There are some concerns that an impurity in the acetone (or methanol) might cause the color change and not the acetone or methanol. Both acetone and methanol are used as solvents for $KMnO_4$ used in organic oxidation reactions, and acetone and methanol may be more difficult to oxidize by permanganate than they appear to be.

2.1.4.6.5 Colorimetric VOC Indicator options for hard-to-oxidize VOCs

The methods for ESLI indication listed in the following sections were not investigated by TDA. They represent possible directions for future research efforts.

2.1.4.6.5.1 Cerium nitrate for oxidation

As an alternative colorimetric indicator, cerium nitrate, suggested in the proposal does not exceed the oxidation potential of MnO_4^{-1}, and there is low probability that the cerium-based color indicators with lower oxidation potentials will function as colorimetric indicators with these refractory organic solvents. The ion, Ce^{4+}, is a strong one-electron oxidizing agent. In terms of its redox potential (E° ~ 1.61 V vs. N.H.E.) it is even a stronger oxidizing agent than Cl_2 (E° ~ 1.36 V) or perchlorate. Few shelf-stable reagents are stronger oxidants. In the redox process Ce(IV) is converted to Ce(III), a one-electron change, signaled by the fading of the solution color from orange to a pale yellow (providing that the substrate and product are not strongly colored). However, cerium nitrate absorbs at 335, 595, 640 and 675 nm and photochemically reacts to form highly reactive $\cdot NO_3$ radicals. Thus cerium indicators, like permanganate are best stored in the dark before use.

2.1.4.6.5.2 Nano-gold catalysts for oxidation

However, hydroxyl radicals, $\cdot OH$, which can be produced from dissociation of hydrogen peroxide, $H_2O_2 \rightarrow 2\cdot OH$, posses an oxidation potential of 2.76 eV in the reaction: $\cdot OH + H^+ + e^{-1} = H_2O$. Peroxide radicals can, in principle, be generated by nanogold catalysts, which operate at room temperature and possess peroxide species on their surfaces: $Au\text{-}O\text{—}OH \rightarrow \cdot OH$.

2.1.4.6.5.3 Nano-gold for ESLI via surface-plasmon resonance

While it might be possible to use nanogold catalysts to oxidize the organic species of interest that remain inert to permanganate. Nanogold can change its color with adsortion of even sub-monolayers of impurities due change in plasmon frequencies. Thus nanogold color changes might provide an option for detecting, by colorimetric means, the difficult-to-oxidize organic solvents.

2.1.4.6.5.4 Two dimensional arrays of spheres

Another option for color change involves changes in structural colors and geometrical-optical interference effects of close-packed nano-spheres that swell or contract as organic vapors are absorbed or as surface-plasmon resonance frequencies are altered by adsorption.

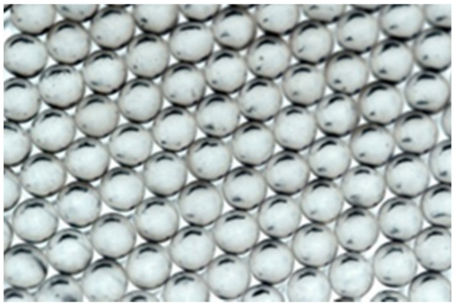
Figure 30. Silica spheres as in synthetic and natural opal

Self-assembled arrays of polystyrene spheres can be deposited onto suitable substrates to produce iridescent colors (see, for example, Patoka and Giersig, 2011, Patoka, 2011; Cong, et al., 2013). Figure 30 shows silica spheres arrayed as they would be exist in opal, which shows interference colors. Figure 31 shows examples of close-packed polystyrene spheres. Interference colors depend upon sphere size and spacing.

In principle, if the array of polystyrene spheres shrinks, swells, or is disrupted, its color would change. It is significant that many of the solvents of interest in the ESLI project that cannot be oxidized by permanganate or cerium compounds are excellent solvents for polystyrene. Thus, these solvents should readily absorb into the spheres. If enough

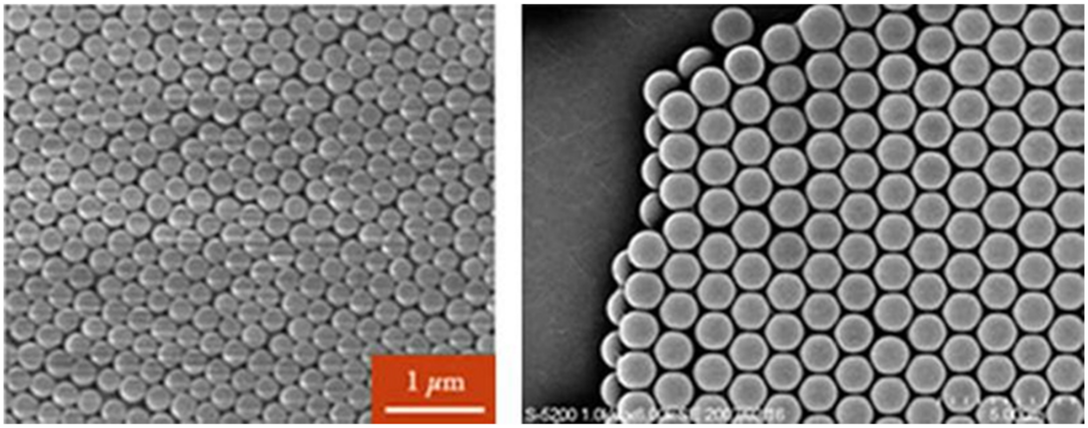

Figure 31. Close-packed, self-assembled arrays of polystyrene spheres exhibit interference colors that are produced by the same principle as the colors seen in opals, swelling or contraction of beads due to adsorption of solvent causes color change

absorbed, and if the sphere size or packing distance changed, then the color would change. At ppm levels, it might require some time before sufficient solvent was absorbed and color change was detected; quantitative measurements would need to be made to confirm this technique's relevance to the time scales and TIC concentrations involved in ESLI.

2.1.4.6.5.4.1 Solvents that swell polystyrene

Aromatic hydrocarbons. Some aromatic hydrocarbons that are excellent solvents for polystyrene include ***benzene, toluene, xylene, and ethylbenzene***. Many of these compounds are toxic, and are some of the widest-spread industrial pollutants, for which respirator protection would certainly be desired.

Chlorinated Aliphatic Hydrocarbons. Many chlorinated aliphatic hydrocarbons also dissolve polystyrene. Common chlorinated aliphatic hydrocarbons that act as solvents for polystyrene include: *methylene chloride, chloroform, and carbon tetrachloride.*

Other Solvents. There are other chemicals and compounds that are excellent solvents for polystyrene. These include *pyridine, acetone, dioxane, dimethylformamide, methyl ethyl ketone, diisopropyl ketone, cyclohexanone, tetrahydrofuran, n-butyl phthalate, methyl phthalate, ethyl phthalate, tetrahydrofurfuryl alcohol, ethyl acetate, butyl acetate, 1-nitro-propane, carbon disulfide, tributyl phosphate, cyclohexane, methylcyclohexane, and ethycyclohexane.* Many of these are of great interest to respirator manufacturers.

2.1.4.6.5.4.2 Solvents Not for Use with Polystyrene

The aliphatic hydrocarbons that do not act as solvents for polystyrene include butane, pentane, hexane, and iso-oxane. Three common alcohols that do not act as solvents are methanol, ethanol, and propanol. Fortunately, these alcohols are readily oxidized by permanganate. Other chemicals that do not act as solvents include water, phenol, and ethyl ether.

2.1.4.6.5.5 Predictable variation in plasmon resonance for colorimetric indication

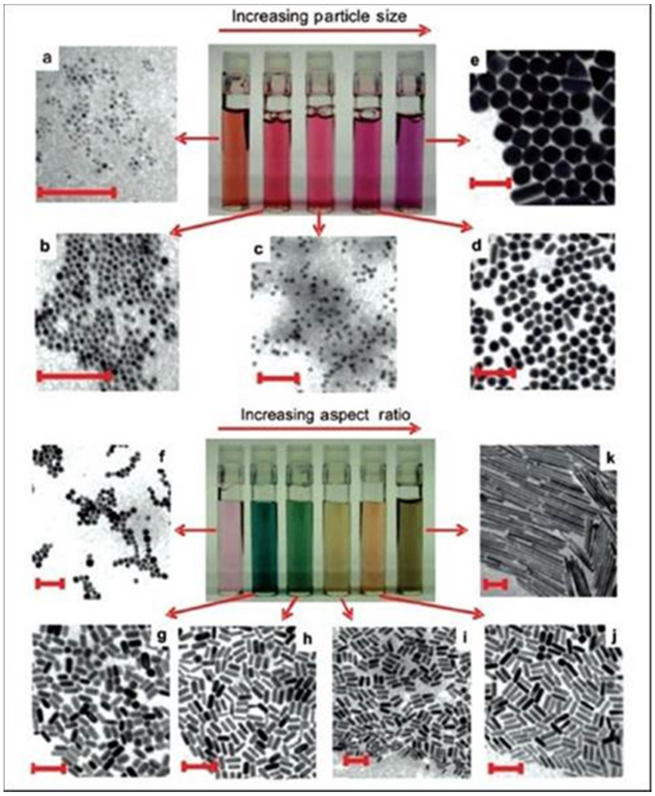

Figure 32. Colors produced by nanomaterials due to plasmon resonance. In principle, sub-monolayer adsorption could change the resonance frequencies and thus the color and form very sensitive colorimetric indicators

Since the submission of the Phase II proposal, 3M has commercialized a colorimetric indicator based upon structural color changes of nanomaterials. The 3M brochure lists the following as detectable by the 3M system and the MIL (Minimum Indication Level) in ppm: isopropanol(650 ppm), benzene(65 ppm), toluene(8 ppm), ethanol(not listed), acetone(not listed), acetonitrile(not listed), dichloromethane(not listed), cyclohexane(not listed), n-hexane(93 ppm), n-pentane(not listed), xylenes(2 ppm), trichloroethylene(TCE)(66 ppm), and methyl-iso-butyl ketone(5 ppm).

Figure 32, taken from the literature, shows examples of nanostructures, which owe their colors to plasmon resonances. In principle, nanomaterials could be used as very sensitive colorimetric indicators, with sub-monolayer adsorption capable of changing the resonance frequency and thus the color. This is beyond the scope of the Phase II work plan, but would provide viable future direction for colorimetric indicators.

2.1.4.6.6 Discussion of results

Permanganate-based VOC indicators are not universal OV detectors. However, they do detect many VOCs. We consider the VOC indicators to be appropriate for commercial use as long as they have a simple disclaimer that lists the VOCs that the indicators do not detect.

The basic vapor indicator shows real promise as commercial ESLI indicator. Its main weakness appears to be its reliance on the availability of water for colorimetric indication. If it is allowed to dry, it becomes too insensitive to act as an ESLI indicator. Fortunately, storage in a sealed bag would solve the moisture issue during storage and there are few environments with RHs below 20%. We consider the basic vapor formulation to be commercially viable.

The acidic vapor indicators suffered an unknown decomposition during the hot diurnal durability conditioning. Given time, it should be relatively simple to identify the decomposition process and take steps to circumvent it. We will continue to work with our commercial partner to complete the acidic indicator's development.

The injection-molded, V3 ESLI-enabled filter cartridge prototypes were an unqualified success. Their construction, cost, and operation were respectively simple, inexpensive, and intuitive. TDA will offer the design to AVON if they chose to move forward with their ESLI development effort.

2.1.4.7 Engineering and cost analysis

This is a cost analysis for adding TDA's ESLI capability to an existing line of carbon bed filter cartridges. The assumptions involved in the cost analysis are listed below.

Table 4. An estimate of the cost to add ESLI capability to an existing filter cartridge

Materials and Labor	**Cost ($/million)**	**Cost/Unit ($)**
Filter paper	$600.00	$0.0006
Gamma Alumina, SA 6176	$3,381.41	$0.0034
No VOC Adhesive	$10,969.70	$0.0110
Brilliant Yellow	$812.00	$0.0008
Bromocresol Purple	$867.00	$0.0009
Sodium Permanganate	$5,000.00	$0.0050
Electricity	$50,000.00	$0.0500
Tooling	$225,000.00	$0.2250
Injection molded parts	$100,000.00	$0.1000
Sub-Total Materials and Utilities		**$0.40**
Labor to assemble and package ESLI modules	$50,000.00	$0.05
Sub-Total Labor		**$0.05**
Total		***$0.45***

- Materials involved in the production of the base filter cartridges (prior to the addition of the ESLI capability) are not included in the cost analysis. *(E.g. activated carbon, HEPA filters, or even the plastic resin that would be used to injection mold ESLI-enabled filter cartridge housings are not part of this analysis because they are existing components of the base cartridge)*

- The ESLI-enabled filter cartridge assembly line would take over an existing filter cartridge assembly line. There are no accommodations in the current cost analysis for the construction of a new facility, assembly line, or for renting additional factory space.

- While this analysis includes the fabrication cost of tooling to produce the ESLI indicator strips, it does not include any of the design costs that would probably be necessary to develop said tooling

The cost/unit price of $0.45 shown in Table 4, factors in the one million part lifecycle of the ESLI tooling. ESLI tooling includes: the mold for the filter cartridge's housing, the mold for the ESLI module, and the mold for the ESLI strip.

Assuming a retail price multiplier of two, the ESLI-enabled filter cartridges would sell for $0.90 more than their base cartridges. Pricing estimates from our commercial partner, AVON, predicted that if ESLI-enabled cartridges could be produced for less than $1 more than current cartridges then the ESLI-enabled cartridges stood a good chance of adoption by large companies that already provide respiratory protection to their employees and have had to establish oversight systems to maintain filter cartridge replacement schedules.

2.1.5 References

Akpan, U.G.; Hameed, B.H. (2009) Parameters Affecting the Photocatalytic Degradation of Dyes Using TiO_2-Based Photocatalysts: A Review, *J. Hazard. Mater.* 170, 520-529.

Avon (2011) Personal communication with Mr. James Wilcox, Business Development Manager, Avon Protection.

Belattar, S.; Debbeche, N.; Segharni, N.; Sehili, T. (2014) Decolorization of Bromocresol Purple (BCP) Photoinduced by a Fe (III) Oxyhydroxide (Goethite), *Sci. Technol. A* 39, 49-60.

Box, G.E.P., Hunter, W.G. and Hunter, J.S. (1978) Statistics for Experimenters, An Introduction to Design, Data Analysis and Model Building, Wiley Interscience.

Box, G.E.P. and Draper, N.R. (1987) Empirical Model Building and Response Surfaces, Wiley

CFR42 Part 84 (2011) "Approval of Respiratory Protective Devices;" electronic Code of Federal Regulations (CFR), data current as of March 21, 2011; available at http://ecfr.gpoaccess.gov/cgi/t/text/text-idx?c=ecfr&sid=f78c67ceae0e938c84443a48d5033159&rgn=div5&view=text&node=42:1.0.1.7.67&idno=42.

CIE (1986) "Colorimetry;" International Commission on Illumination Publication No. 15.2, 2nd Edition.

Cong, Hailin; Yu, Bing; Wang, Shaopeng; Qi, Limin; Wang, Jilei; Ma Yurong (2013) Preparation of Iridescent Colloidal Crystal Coatings with Variable Structural Colors, *Optics Express,* 21(15), 17831, DOI: 10.1364/OE.21.017831.

England, W.G. (1999) "Fiber Filter and Methods of Use Thereof," U.S. Patent 5,942,323, August 24, 1999.

Favas, G. (2005) “End of Service Life Indicator (ESLI) for Respirator Cartridges. Part I: Literature Review,” Human Protection and Performance Division, Defence Science and Technology Organization, Vistoria, Australia.

Fraser, B.; Murphy, C.; Bunting, F. (2004) Real World Color Management, 2nd Ed.; Peachpit Press, Berkeley, CA.

Hanna, G.F.; Kuehner, R.L. (1964) A Chemical Method for Odor Control, *Annals New York Academy of Sciences*,**116**, 663-675.

Hicks, Manuel G., “Method of Minimizing Manganese Dioxide Sludge Formation,” U.S. Patent 4,268,487, May 19, 1981.

Kuehner, Richard L., “*Process for Deodorizing and Sterilizing Air*,” U.S. Patent 2,683,074, July 6, 1954.

Kuehner, Richard L.; Hopkins, Neil E., “*Method of Deodorizing and Sterilizing Air in Enclosed Spaces,*“ U.S. Patent 2,876,507, Mar. 10, 1959.

Lai, Sheng; Lee, Donald G. (2002) Lewis Acid Assisted Permanganate Oxidation, Tetrahedron 58, 9879-9887.

Lee, Donald G.; Chen, Tao; Wang, Zhao (1993) Heterogeneous Permanganate Oxidations. 5. The Preparation of Aldehydes by Oxidative Cleavage of Carbon-Carbon Double Bonds, J. Org. Chem. 58, 2918-2919.

Lee, Donald G.; Moylan, Christopher R.; Hayashi, Takatoshi; Brauman, John I. (1987) Photochemistry of Aqueous Permanganate Ion, J. Am. Chem. Soc. 109, 3003-3010.

Lincoln, R.C.; Osment, H.E. (1965) “Production of Potassium Permanganate Activated Alumina Composite,” U.S. Patent 3,226,332, December 28, 1965.

Livermore, D.M.; Brown, D.F.J. (2001) *J. of Antimicrobial Chemotherapy*, **48**, *Suppl. S1*, 59-64.

Mantell, C.L.; (1951) Adsorption, McGraw-Hill.

McAllister, J.W.; Ord, J.A.; Anders, L.W.; Kohler, G.A. (1979) “Respirator,” U.S. Patent 4,155,358, May 22, 1979.

Misra, Chanakya (1986) *Industrial Alumina Chemicals*, ACS Monograph 184 (American Chemical Society, Washington, D.C.) p. 123.

Montgomery, D.C. (1976) Design and Analysis of Experiments, Wiley.

MSA (2007) “MSA Cartridge Life Expectancy Calculator,” Mine Safety Appliances Company (MSA); available at http://webapps.msanet.com/cartlife/.

MSA (2011) Personal communication with MSA Product Manager.

Nakai, Hiromi; Nakatsuji, Hiroshi (1994) “Mechanism of Photochemical Reaction of Permanganate Ion,” *J. Mol. Struct. THEOCHEM* 311, 141-151.

Nakai, Hiromi; Ohmori, Yutaka; Nakatsuji, Hiroshi (1995) Theoretical Study on the Photochemical Reaction of Permanganate Ion, MnO_4^-, *J. Phys. Chem.* 99(21), 8550-8555.

NIOSH/BLS (2003) “Respirator usage in Private Sector Firms, 2001,” U.S. Department of Labor, Bureau of Labor Statistics (BLS); U.S. Dept. of Health and Human Services, Centers for Disease Control and Prevention, National Institute for Occupational Safety and Health (NIOSH); September, 2003; page 133.

NIST (2010) NIST/SEMATECH e-Handbook of Statistical Methods, http://www.itl.nist.gov/div898/handbook .

North Safety (2011) “Respiratory Protection,” product catalogue, available at https://www.northsafety.com; North Safety (Honeywell) product help-line, personal communication, February 22, 2011.

Ohno, Y. (2000) “CIE Fundamentals for Color Measurements,” paper for IS&T NIP Conference, October 16-20, 2000; Vancouver, Canada.

OSHA (2011) “Respiratory Protection,” in Occupational Safety and Health Standards, Personal Protective Equipment; 29 CFR 1910.134; available at http://www.osha.gov/pls/oshaweb/owadisp.show_document?p_table=STANDARDS&p_id=12716#1910.134.

Patoka, Piotr [2011] Tunable Plasmonic Properties of Nanostructures Fabricated by Shadow Nanosphere Lithography, Disseration, Freie Universität Berlin.

Patoka, Piotr; Giersig, Michael (2011) Self-Assembly of Latex Particles for the Creation of Nanostructures with Tunable Plasmonic Properties, *J. Mat. Chem.* 21 16783-16796,

Rose-Pehrsson, S.L.; Williams, M.L. (2005) “Integration of Sensor Technologies into Respirator Vapor Cartridges as End-of-Service-Life Indicators: Literature and manufacturer’s Review and Research Roadmap,” Report # NRL/MR/6112--05-8875, Naval Research Laboratory, Washington D.C., May 6, 2005.

Rutkowski, P.I. (2008) Principle Engineer, Advanced Technology Group, MSA Company; *Personal Communication*.

Snyder, J. (2006) "Update on End-of-Service-Life Indicator Project," Technology Research Branch, NPPTL; available at http://www.cdc.gov/niosh/npptl/researchprojects/pdfs/ESLI%2006272006.pdf.

Snyder, J. (2008) NIOSH Presentation to Peter Rutkowski of MSA Company, November 2008, Pittsburgh, PA.

Snyder J. (2010) "End of Service Life Program for Personal Protective Equipment at NPPTL;" Presentation to the Committee on Personal Protective Equipment for Workplace Safety and Health, Board on Health Sciences Policies, Institute of Medicine of the National Academies, October 8, 2010.

Tavakkoli, Haman; Ghaemi, Arezoo; Mostofizadeh, Mastaneh (2014) Syntheis and Evaluation Catalytic Efficiency of Perovskite-Type Oxide Nanopowders in Removal of Bromocresol Purple from Aqueous Solution, *Int. J. Sci. Research Knowledge* 2(7) 340-351.

Werfers, Karl; Misra, Chanakya (1987) *Oxides and Hydroxides of Aluminum* (Alcoa Laboratories, Pittsburgh).

Whatman® (2010) "Qualitative Filter Papers – Standard Grades; Grade 4: 20-25 µm;" available at http://www.whatman.com/products.aspx?PID=1.

Wolfe, Saul; Ingold, Christopher F. (1983) Oxidation of Organic Compounds by Zinc Permanganate, *J.Am.Chem.Soc.* 105(26) 7755-7757.

2.1.6 Appendix I: Description of the CIE L a b Color Space

The CIE L a b system, the most complete color space specified by the International Commission on Illumination (Commission Internationale d'Eclairage, hence "CIE"), quantitatively describes all the colors visible to the human eye and was created to serve as a device independent model to be used as a reference (CIE, 1986). To evaluate a color change, a handheld colorimeter is used to measure a color both before and after it changes, and then using the CIE L a b color system, a quantitative value for a "color change" can then be calculated. Using the colorimeter and the CIE L a b color system, the indicator colors observed were evaluated quantitatively and we were thus able to perform statistical analyses on the resulting calculated color changes to evaluate variables such as color-change reproducibility, lightness and darkness of the colors produced, and the total color difference before and after test vapor exposure.

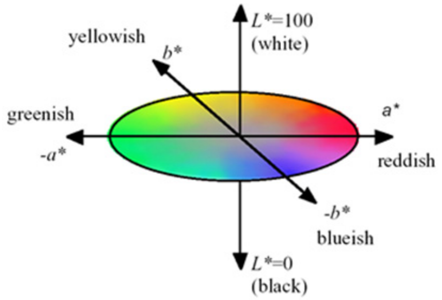

Figure 33. CIE L a b color space (Ohno, 2000)

The CIE L a b -system measures color in 3 dimensions (Figure 33), L , a , and b , where L = 0 yields black and L = 100 indicates diffuse white, a = negative values indicate green while positive values indicate magenta, and b = negative values indicate blue and positive values indicate yellow. In addition, by obtaining values for L , a , and b for two different colors, the color difference, ΔE_{ab} , can be calculated according to Equation 1. (The magnitude of a color change calculated from Equation 1 is simply the distance between two color points, each with coordinates of L , a , and b , in the CIE L a b 3-dimensional color space shown in Figure 33.) Using this system, ΔE_{ab} values ≥ 2.3 represent a noticeable difference between two colors for the human eye (Fraser, 2004).

Equation 1. Formula for calculating the magnitude of a color change in the CIE L a b 3-dimensional color space.

$$\Delta E^{*}_{ab} = \sqrt{(\Delta L^{*})^{2} + (\Delta a^{*})^{2} + (\Delta b^{*})^{2}}$$

Using a handheld colorimeter, the color of each indicator test band was measured before and after vapor exposure. The values of L , a , and b were recorded, and with this data, ΔE_{ab} was calculated from Equation 1 and used to evaluate the magnitude of the color difference for indicators before and after exposure to the vapor at different concentrations, temperatures, and relative humidities. Though many sources say that color changes as low as $\Delta E_{ab} \geq 2.3$ can be detected by the human eye (Fraser, 2004), TDA has found that $\Delta E_{ab} \geq 10$ are more reasonably seen and we therefore used this value as the lower limit for a detectable color change in our studies.

Appendix I References

CIE (1986) "Colorimetry;" International Commission on Illumination Publication No. 15.2, 2nd Edition.

Fraser, B.; Murphy, C.; Bunting, F. (2004) Real World Color Management, 2nd Ed.; Peachpit Press, Berkeley, CA.

Ohno, Y. (2000) "CIE Fundamentals for Color Measurements," paper for IS&T NIP Conference, October 16-20, 2000; Vancouver, Canada.

2.2 Publications

No publications resulted from this grant support.